Photocatalytic product-selective reduction of CO_2, CO and carbonates

Rohan Bhimpuria, Monika Tomar, Anders Thapper, Eszter Borbas*

Department of Chemistry, Ångström Laboratory, Box 523, Uppsala University, Uppsala, Sweden

eszter.borbas@kemi.uu.se

Table of Contents

Materials and methods

Compounds **SmL**,[1] **EuL**,[1] **GdL**,[1] BIH[2] and BI(OH)H[3] were synthesized following literature methods. All other chemicals were from commercial sources and used as received. SmI_2 (0.1 M in THF), $Sm_2CO_3 \cdot H_2O$, formic acid, ferrocene (Fc), $^{13}CO_2$, $NaH^{13}CO_3$, *N*,*N*-diisopropylethylamine (DIPEA), triethylamine (TEA), triethanolamine (TEAO), and 1,8-diazabicyclo[5.4.0]undec-7-ene (DBU) were purchased from Sigma-Aldrich. DMF and MeCN were obtained from an Inert Puresolv solvent purification system. ^{1}H NMR (400 MHz) and ^{13}C NMR (101 MHz), spectra were recorded on a JEOL 400 MHz instrument. Chemical shifts were referenced to residual solvent peaks and are given as follows: chemical shift (δ, ppm), multiplicity (s, singlet; br, broad; m, multiplet), coupling constant (Hz), integration. The reactions were monitored by headspace GC-MS Thermal Trance 1300 with FID detector and carrier gas is Ar and H_2, where the Ar flow is 350 mL/min, and the H_2 flow is 30 mL/min. Detector temperature is 250 °C, oven temperature is 60 °C to 110 °C with a ramp of 10 °C/min. All spectroscopic measurements were performed in MeCN and DMF (taken from the solvent purification system) unless indicated otherwise. Quartz cells with 1 cm optical pathlengths were used for the room temperature measurements. All emissions were corrected by the wavelength sensitivity (correction function) of the spectrometer. IR spectra was recorded on a dry sample by making a pellet using KBr with the analyte (100:1). Blank was recorded with only KBr pellet.

Synthesis of L^{Me}

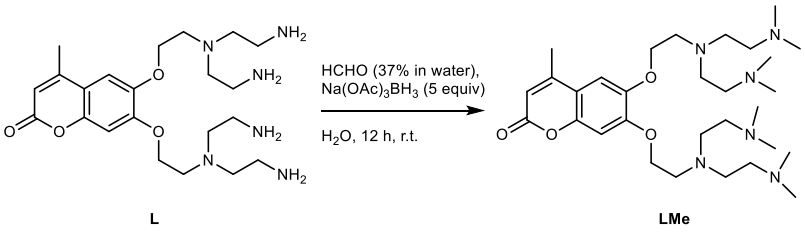

Scheme S1. Synthesis of L^{Me}.

To a stirred solution of **L** (100 mg, 0.22 mmol, 1.0 equiv) in H_2O (1 mL), formaldehyde (0.5 mL, 25% in water) was added. The mixture was stirred for 1 h, after which $NaBH(OAc)_3$ (235 mg, 1.10 mmol, 5.0 equiv) was added. The resulting solution was stirred at r.t. for 24 h. The progress of the reaction was monitored using LC-MS. Upon completion of the reaction the crude product was purified by neutral alumina column chromatography using MeOH in CH_2Cl_2 (2%→50%) as an eluent. The evaporation of the solvents and drying of the residue under vacuum yielded a pale yellow solid (85 mg, 69%). ^{1}H NMR (400 MHz, D_2O) δ 6.98 (s, 1H), 6.87 (s, 1H), 6.03 (s, 1H), 4.65 (s, 6H), 4.52 (s, 6H), 4.10 (m, 4H), 3.43 (m, 2H), 2.89 (m, 4H), 2.57 (m, 16H), 2.25 (s, 3H), 2.18 (s, 12H); ^{13}C NMR (101 MHz, D_2O) δ 164.5, 156.1, 151.2, 148.7, 144.7, 113.1, 110.8, 107.6, 101.3, 81.7, 79.9, 71.6, 69.8, 66.9, 54.7, 51.0, 50.8, 50.2, 48.5, 46.6, 46.4, 44.7, 43.1, 37.1, 34.5, 32.9, 22.8, 18.4; HRMS (ESI, *m/z*) calcd for $C_{30}H_{54}N_6O_4H$ [$M+H^+$] 563.4284, found 563.4279.

Reaction optimization and control reactions

General procedure. A vial containing a solution of **LnL** (1 mM – 1 μM) in MeCN (2 mL), sacrificial donor (1-20%v/v), proton source (0.4 mL), was saturated with CO_2 for 15–20 mins. Then, the solution was irradiated in an EvoluChem PhotoRedOx Box™ for 16 h using a 40 W blueLED lamp (Kessil A160WE Tuna Blue, λ_{max} = 463 nm) at room temperature. After that gaseous phase samples were subjected to headspace GC-MS analysis while liquid phase samples were subjected to NMR analysis. Results are the average of 3 independent experiments.

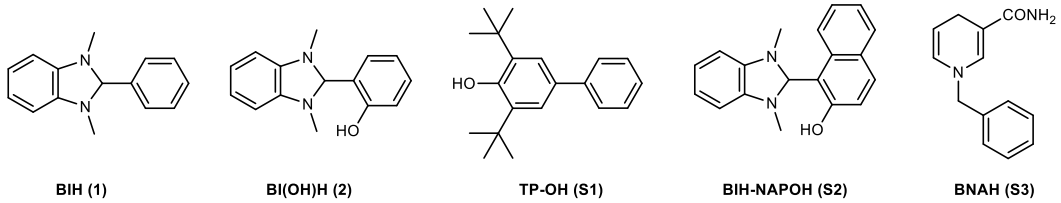

Figure S1. Structures of sacrificial donors used in this study.

Table S1. Optimisation reactions for selective CO formation.[a]

Entry	Catalyst (conc.)	Sacrificial donor	Additive	TON_{CO}	TON_{HCOOH}	TON_{H2}
1	**SmL** (1 mM)	DIPEA (10 eq)	LiCl, H_2O	-	-	-
2	**SmL** (1 mM)	DIPEA	LiCl, H_2O	65	-	-
3	**SmL** (1 mM)	DIPEA	H_2O (20%v/v)	70	-	-
4	**SmL** (1 mM)	DIPEA	-	0	-	-
5	**SmL** (1 mM)	DIPEA	H_2O (50%v/v)	10	-	-
6	**SmL** (1 mM)	TEA	H_2O (20%v/v)	30	-	-
7	**SmL** (1 mM)	TEAO	H_2O (20%v/v)	10	-	-
8	**SmL** (1 mM)	DBU	H_2O (20%v/v)	30	-	-
9	**SmL** (1 mM)	DIPEA	Trifluoroethanol	10	-	-
10	**SmL** (100 μM)	DIPEA	H_2O (20%v/v)	800	-	-
11	**SmL** (10 μM)	DIPEA	H_2O (20%v/v)	31000	-	-
12	**SmL** (1 μM)	DIPEA	H_2O (20%v/v)	378000	-	-

[a] Reactions were performed in a CO_2-saturated solution of MeCN:DIPEA (4:1) with the indicated catalyst loading and in the presence of indicated additive under blue LED irradiation for 16 h.

Table S2. Optimization reactions for selective formate formation.[a]

Entry	Catalyst (conc.)	Sacrificial donor	Additive	TON_{CO}	TON_{HCOOH}	TON_{H2}
1	**SmL** (1 mM)	DIPEA (10 eq)	Benzoic acid	20	-	-
2	**SmL** (1 mM)	DIPEA (10 eq)	Sodium citrate	20	-	-
3	**SmL** (1 mM)	DIPEA (10 eq)	Phloroglucinol	5	-	-
4	**SmL** (1 mM)	BNAH (1 M)	H_2O (20%v/v)	60	-	-
5[b]	**SmL** (1 mM)	BIH (1 M)	H_2O (20%v/v)	90	2500	2
6[b]	**SmL** (100 μM)	BI(OH)H (1 M)	H_2O (20%v/v)	10	2200	-
7	**SmL** (100 μM)	BIH-NAPOH (1 M)	H_2O (20%v/v)		-	
8	**SmL** (100 μM)	TP-OH (0.2 M)	H_2O (20%v/v)	-	150	-

[a] Reactions were performed in a CO_2-saturated solution of MeCN:DIPEA (4:0.5) with the indicated catalyst loading and in the presence of indicated additive under blue LED irradiation for 16 h. [b] Reaction mixtures were irradiated for 72 h.

Table S3. Reactions of CO and formic acid.[a]

Entry	Substrate	Catalyst (conc.)	Sacrificial donor	TON_{CH3OH}	TON_{CH4}	TON_{H2}
1	CO	**SmL** (1 mM)	DIPEA (1 M)	-	-	-
2	CO	**SmL** (1 mM)	DIPEA (1 M)	-	70	-
3	CO	**SmL** (100 µM)	BI(OH)H (1 M)	90	-	1000
4	HCOOH	**SmL** (1 mM)	DIPEA (1 M)	-	-	-
5	HCOOH	**SmL** (1 mM)	BI(OH)H (1 M), DIPEA (1 M)	-	-	-
6	-	**SmL** (100 µM)	**2**, DIPEA (1 M)	-	-	14000

[a] Reactions were performed in a CO- (entries 1–3) or Ar- (entries 4 and 5) saturated solution of MeCN:DIPEA (4:1) (entry 1) or DMF:DIPEA (4:1) (entries 2–6) with the indicated catalyst loading and with a water content of 50% v/v under blue LED irradiation for 48 h. Note: reaction did not work at **SmL** concentration lower than 1 mM.

Table S4. Control reactions.[a]

Entry	Gas	Catalyst (conc.)	Sacrificial donor	TON_{CO}	TON_{HCOOH}	TON_{H2}	TON_{CH3OH}	TON_{CH4}
1	CO_2	**GdL** (1 µM)	DIPEA	2	-	-	-	-
2	CO_2	-	DIPEA	-	-	-	-	-
3	CO_2	-	**1**, DIPEA	0	-	-	-	-
4	CO_2	-	**2**, DIPEA	7	2	-	-	-
5[b]	CO_2	**SmL** (1 µM)	DIPEA	0	-	-	-	-
6	CO	**SmL** (1 mM)	-	-	-	-	-	-
7	Ar	**SmL** (1 mM)	DIPEA	-	-	-	-	-
8	Ar	**SmL** (100 µM)	**2**	-	-	800	-	-
9	Ar	**GdL** (100 µM)	**2**, DIPEA	-	-	1450	-	-

[a] Reactions were performed in a gas-saturated solution of MeCN (entry 1-5), DMF (6-9) with the indicated catalyst and catalyst loading, and containing H_2O (20% v/v) and/or organic hydride (1 M) (when listed). Irradiation took place with a blue LED; [b] Reaction was carried out in the dark.

Table S5. Concentration-dependent reactivity of $SmCl_3$:L mixture.[a]

Entry	Catalyst (conc.)	Time (h)	TOF_{CO}
1	$SmCl_3$ (1 µM) + **L** (1 µM)	16	46941
2	$SmCl_3$ (1 µM) + **L** (10 µM)	8	47191
3	$SmCl_3$ (1 µM) + **L** (100 µM)	7	53932

[a] Reactions were performed in a CO_2-saturated solution of MeCN:DIPEA (4:1) containing $SmCl_3$ and **L** in the indicated amounts, as well as H_2O (20% v/v). Irradiation was with blue LED. TOF was calculated using equation TOF = (TON_{CO})/ Time (h) after which catalysis was no longer occurring.

Reference GC-MS traces

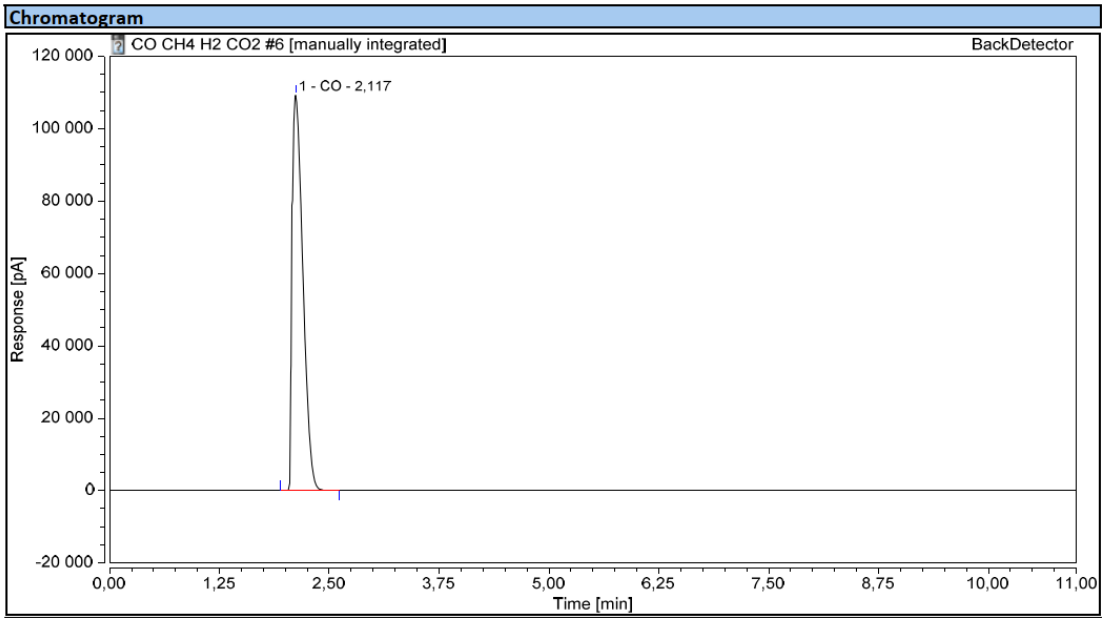

Figure S2. Reference GC-MS trace of CO.

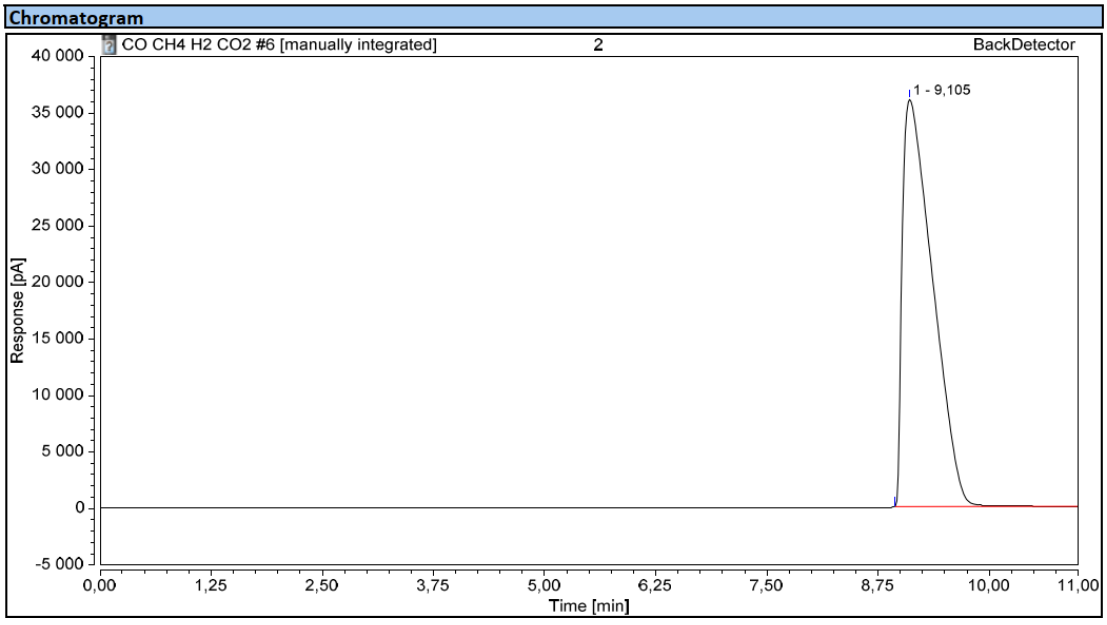

Figure S3. Reference GC-MS trace of CO_2.

Catalyst stability

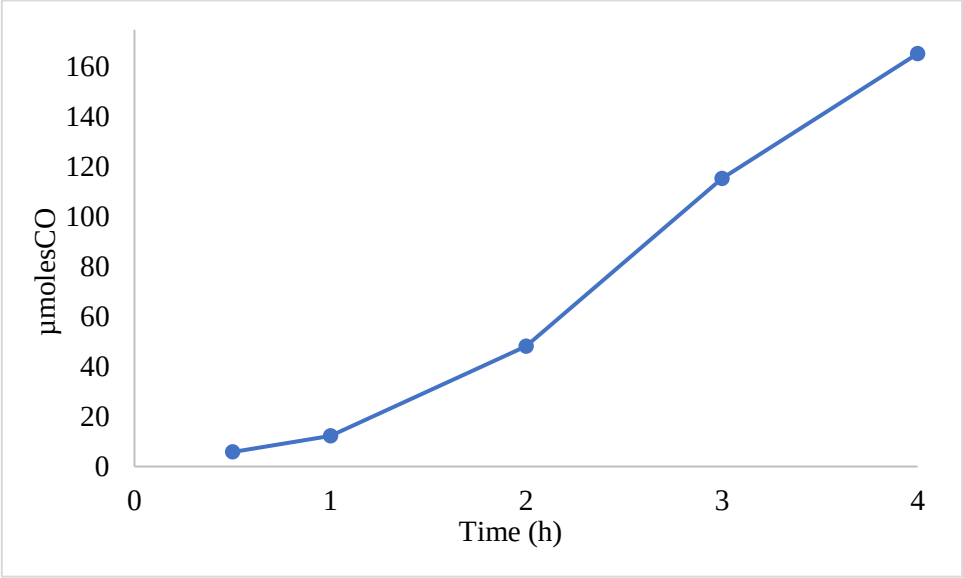

Figure S4. Initial progress of reactions in a solution containing **SmL** (1 µM) and saturated with CO_2 in MeCN:DIPEA (4:1) containing water (20% v/v) at different time intervals. The reaction was irradiated with blue LED.

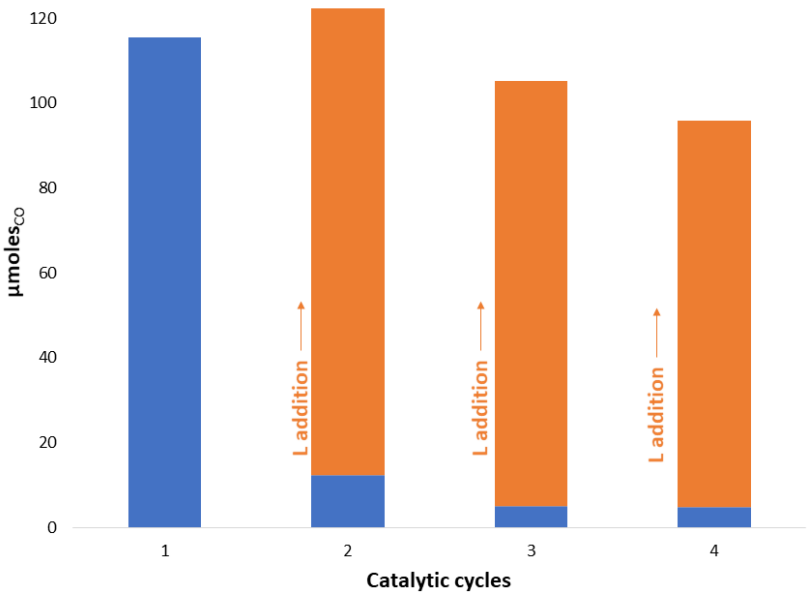

Figure S5. Evaluation of catalyst regeneration by examining catalytic activity after each 16 h by purging with CO_2 a solution of **SmL** (1 µM) in MeCN:DIPEA (4:1) and water (20% v/v) and irradiating it with blue LED for 16 h each time (blue bars); and upon the addition of **L** after each 16 h. **L** addition recovers the **SmL** catalytic activity (orange bars) indicating degradation of **L** may be the reason for the loss of catalytic activity.

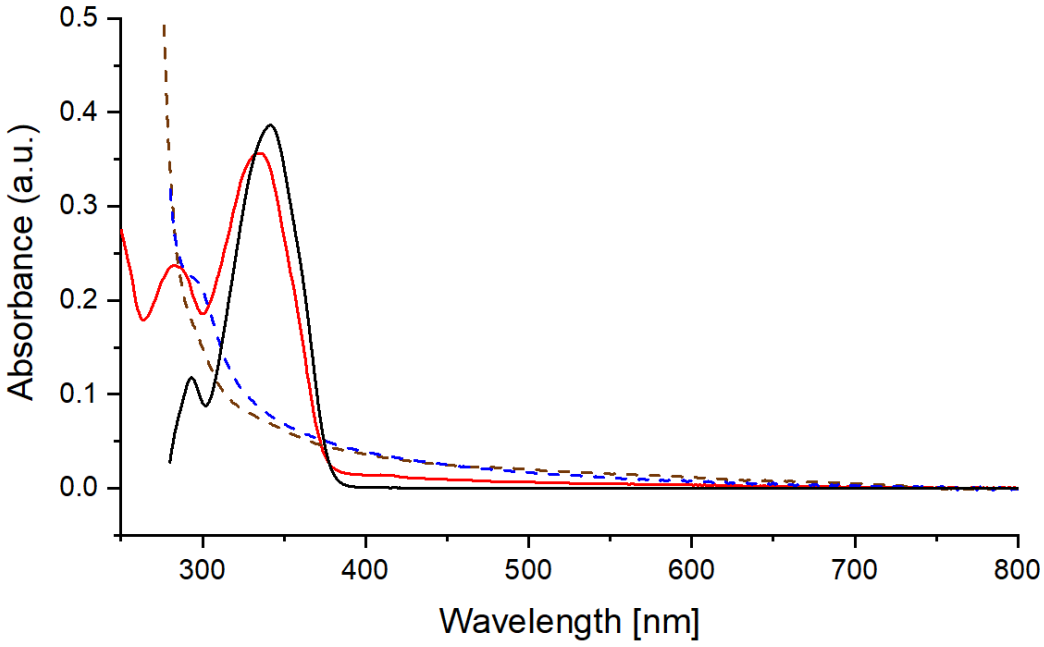

Figure S6. Absorption spectra of **L** in DMF (black line) and **SmL** + diethylcarbonate (red line) and the reaction mixtures after 16 h in the optimized condition, **SmL**+ diethylcarbonate (brown dotted line) and the mixture of $SmCl_3$ and **L** (blue dotted line) in MeCN. [**SmL**: 50 µM, diethylcarbonate: 80 µM in MeCN and 20% H_2O].

Study of reaction intermediates

1. **Study of reactivity of carbamate intermediate with SmL**

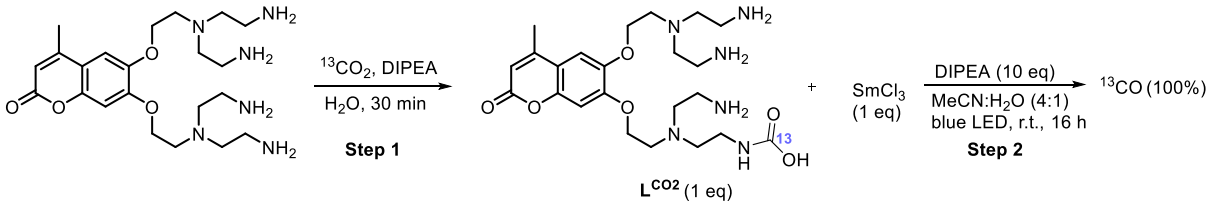

Scheme S2. Synthesis of the ^{13}C-labelled analogue of L^{CO2}, and its reactivity.

Step 1. A solution of **L** (10 mg, 0.022 mmol, 1.0 equiv) in H_2O (1 mL) and DIPEA (0.5 mL) was saturated with $^{13}CO_2$. The mixture was stirred for 30 min. The reaction progress was monitored by ^{13}C NMR spectroscopy, which showed a strong carbamate peak corresponding to NH-$^{13}CO_2^-$. $\mathbf{L^{CO2}}$ could not be isolated as such since it quickly releases CO_2 upon drying. Therefore, an aq. HCl solution was added to the reaction mixture. Evaporation of the solvents and drying of the residue under vacuum yielded a pale-yellow solid as a mixture of the HCl salt of $\mathbf{L^{CO2}}$ and of DIPEA. ^{1}H NMR (400 MHz, D_2O) δ 6.82 (m, 2H), 5.95 (s, 1H), 4.08–4.03 (m, 4H), 2.92–2.84 (m, 13H), 2.74–2.69 (m, 8H); ^{13}C NMR (101 MHz, D_2O) δ ^{13}C NMR (101 MHz, D_2O) δ 164.6, 161.3, 156.1, 151.3, 148.5, 144.8, 130.3, 112.8, 110.6, 106.9, 66.7, 63.2, 52.9, 51.7, 45.1, 18.3.; HRMS (ESI, *m/z*) calcd for $C_{23}H_{40}Cl_2N_6O_6$ [M+H$^+$] 566.2398, found 566.2391.

Step 2. To a vial containing a solution of $\mathbf{L^{CO2}}$ (1 mM), DIPEA (10 eq) in MeCN:H_2O (2:0.5 mL), $SmCl_3$ (1 mM) was added. The solution was purged with Ar for 20 min, after which it was irradiated for 16 h with blue LED. The reaction mixture was analysed using GC-MS and ^{13}C NMR spectroscopy showing presence of ^{13}CO (*m*/*z* = 29) and the complete disappearance of NH-$^{13}CO_2^-$ peak.

*Note: **Steps 1** and **2** could also be performed in one pot, and the result was same.*

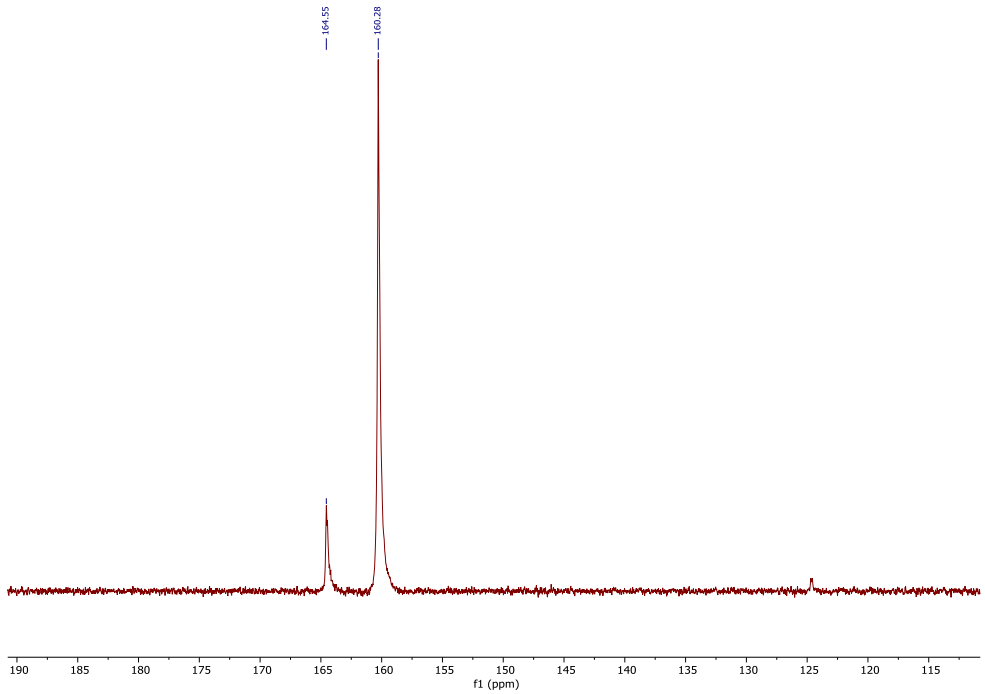

Figure S7. ^{13}C NMR spectrum of a $^{13}CO_2$-purged solution of water:DIPEA (4:1) containing **L** after 30 min, showing the presence of carbamate (δ = 164.5 ppm) and inorganic carbonate (δ = 160.2 ppm). The results indicate the formation of $\mathbf{L}^{\mathbf{CO2}}$ before irradiation.

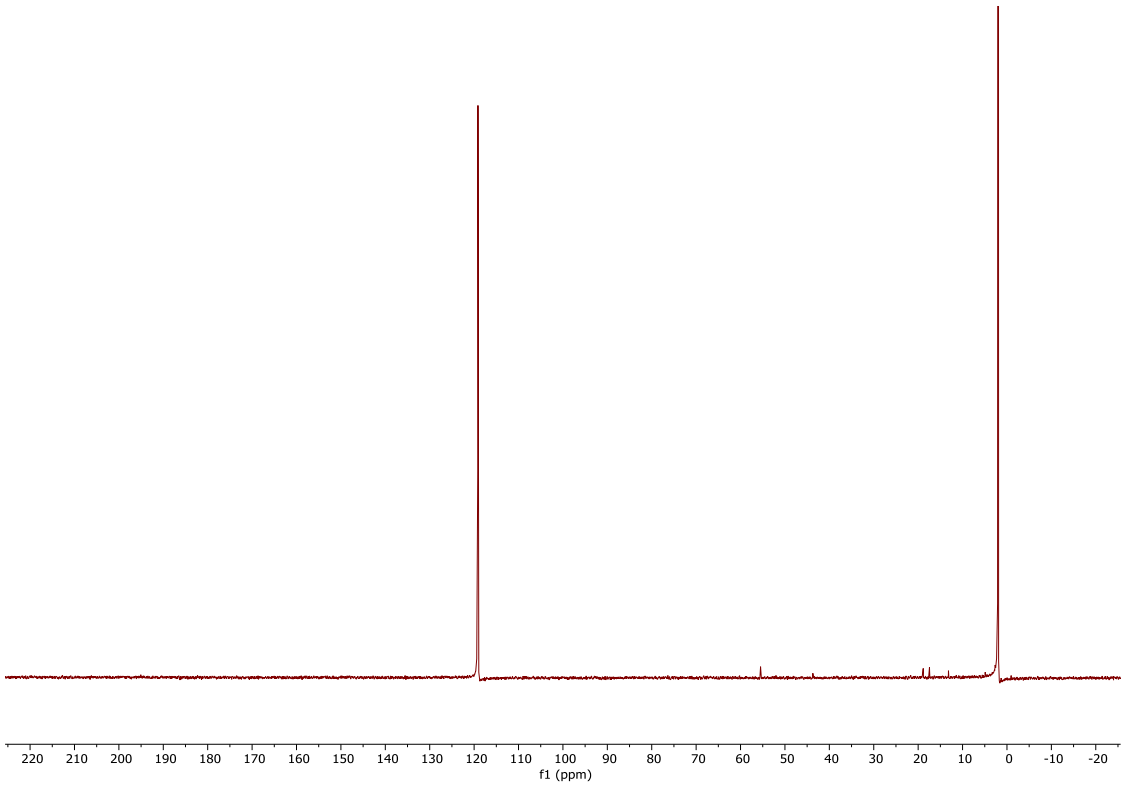

Figure S8. ^{13}C NMR spectrum of an Ar-saturated solution of MeCN: water (20% v/v) containing equimolar mixture of $\mathbf{L}^{\mathbf{CO2}}$ (1 mM): $SmCl_3$(1 mM) after 16 h irradiation. It shows disappearance of carbamate (δ = 164.5 ppm) peak.

2. **Study of the reaction of HCO_3^- with SmL**

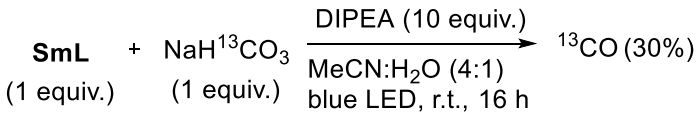

Scheme S2. Stoichiometric reaction between SmL and $NaHCO_3$.

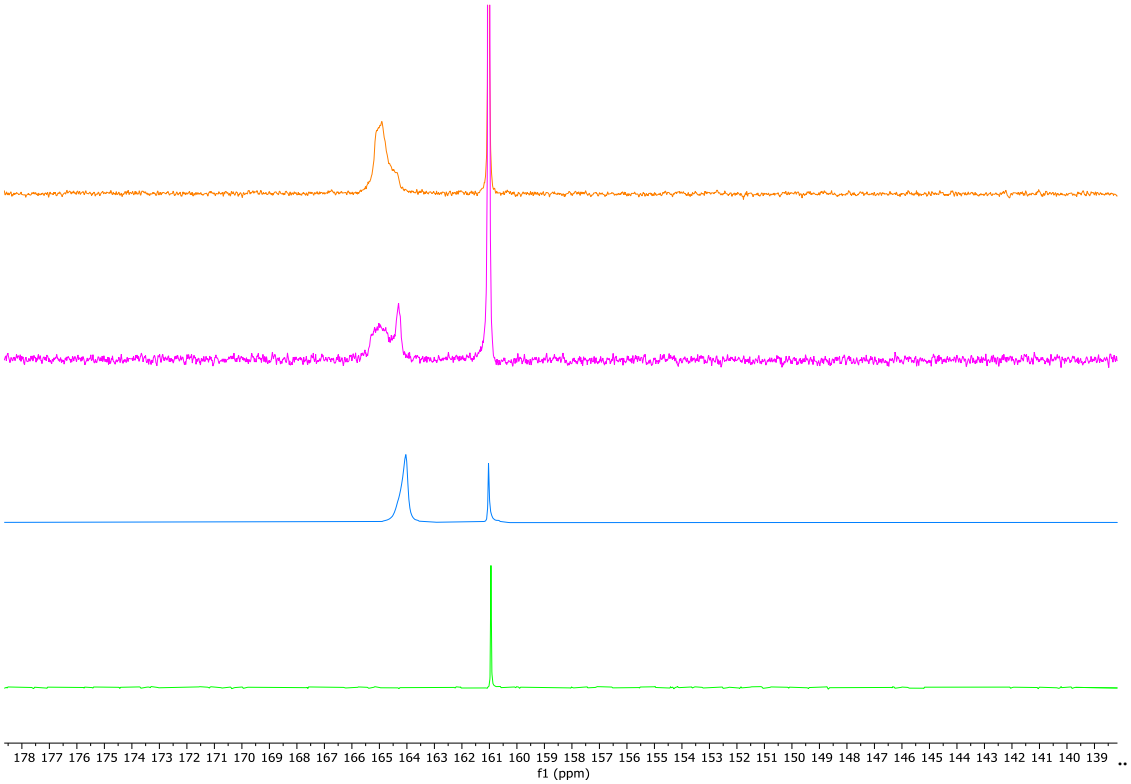

Figure S9. ^{13}C NMR spectrum of a solution of water:DIPEA (4:1) and $NaH^{13}CO_3$ (1 mM) containing orange: $SmCl_3$ and **L** (1 mM each); magenta: $SmCl_3$ (1 mM); blue: **SmL** (1 mM) during blue LED irradiation; green: **SmL** (1 mM) after irradiation. *The broad peak at δ = 164.9 ppm is due to* ***(SmL)$_2$CO$_3$****,* ***SmL^{CO2}*** *is found at δ = 164.1 ppm, and* ***HCO_3^-*** *at δ = 160.9 ppm.*

3. **Study of the reactivity of $(SmL)_2CO_3$**

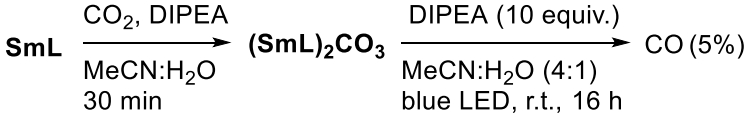

Scheme S3. $(SmL)_2CO_3$ and its reactivity.

$(SmL)_2CO_3$. A solution of **SmL** (10 mg, 0.014 mmol, 1.0 equiv) in MeCN:DIPEA:H_2O (4:1:0.8 mL) was purged with CO_2 for 20 min, after which a white precipitate started to form. The reaction mixture was stirred for a further 30 min. The evaporation of the solvents and the drying of the residue under

vacuum yielded a colorless solid (20 mg, 95%). IR ν (cm^{-1}) = 3317, 2935, 2663, 1633, 1494, 1425, 846. $(SmL)_2CO_3$ prepared alternatively from the reaction of Sm_2CO_3 and L also gave the same results.

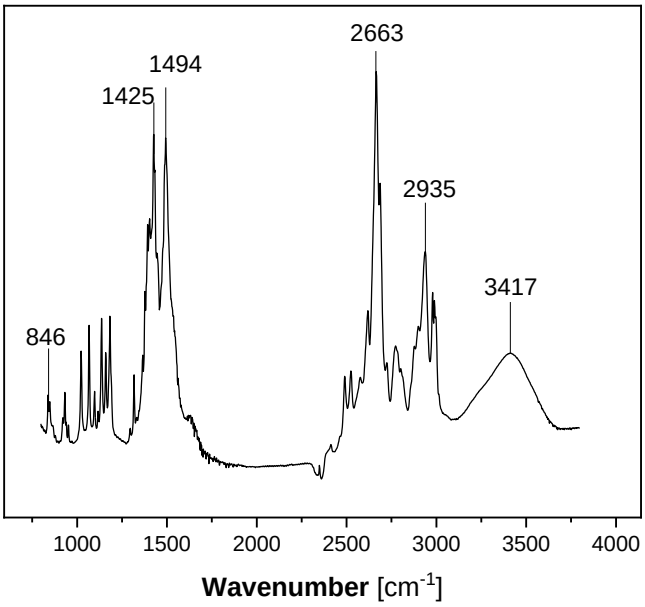

Figure S10. FT-IR spectrum of the reaction mixture of a CO_2-saturated solution MeCN:H_2O:DIPEA (4:1:0.8), SmL (1 mM) **before irradiation**. Spectrum recorded as KBr pellet. It shows a peak at ν_{as}(CO) = 1494 cm^{-1}; δ_m (CO) = 846 cm^{-1} due to **$(SmL)_2CO_3$**. *The ν_{as}(CO) = 1494 cm^{-1} peak is 29 cm^{-1} blue-shifted in comparison to K_2CO_3 ν_{as}(CO) = 1465 cm^{-1} (Ref. [4]) and matches commercially available Sm_2CO_3 (below). Peaks in the regions 2500–3000 and 1000-1200 cm^{-1} belong to **L**.*

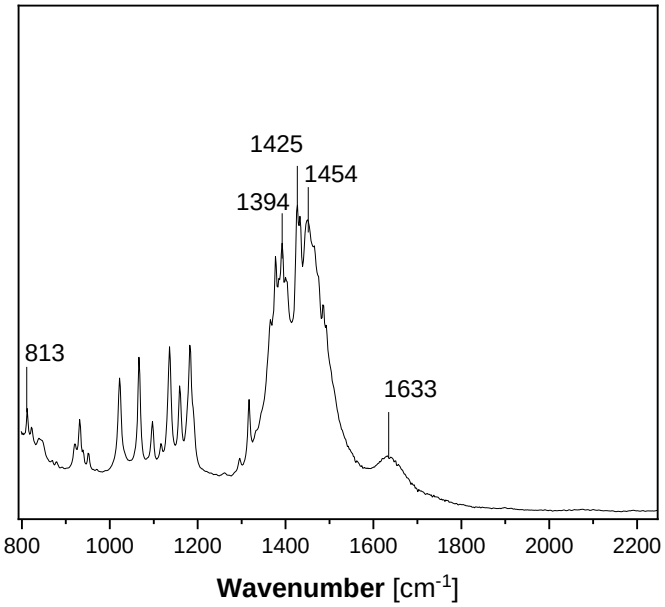

Figure S11. FT-IR spectrum of a KBr pellet of **$(SmL)_2{}^{13}CO_3$**. The peak at $\nu_{as}(^{13}CO)$ = 1454 cm^{-1} is *red-shifted in comparison to* **$(SmL)_2CO_3$**; δ_m (^{13}CO) = 816 cm^{-1} is also *red-shifted*. This further confirms the formation of **$(SmL)_2CO_3$**.

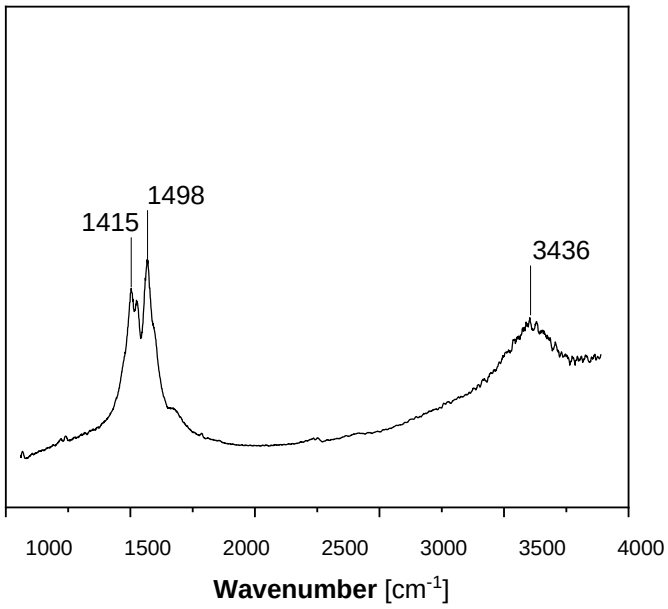

Figure S12. FT-IR spectrum of a KBr pellet of commercially available $Sm_2CO_3 \cdot H_2O$.

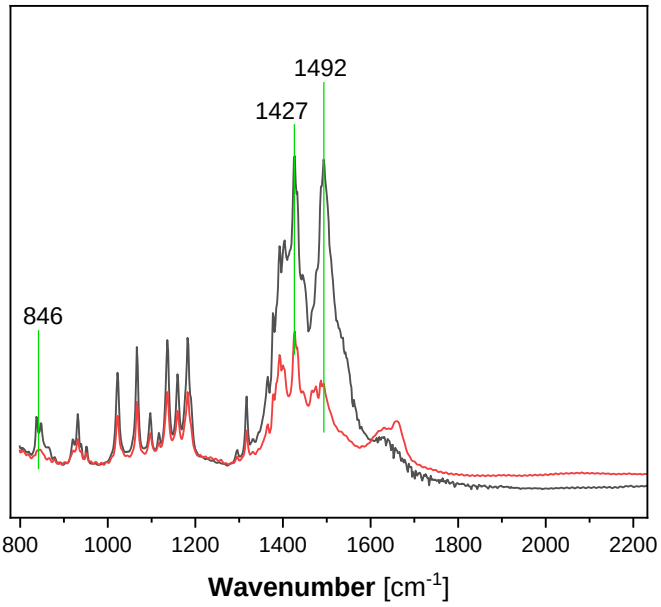

Figure S13. FT-IR spectrum of a KBr pellet of **[(SmL)$_2$CO$_3$]** before (black) and after (red) irradiation with blue LED for 16 h. It shows the reduction in intensity of peak at ν_{as}(CO) = 1492 cm^{-1} due to reduction to CO.

Carbonate reduction reactions using SmL

Table S6. Reactions with different carbonates.[a]

No.	CO_2 source	Catalyst (conc.)	Sacrificial donor	$\mu moles_{CO}$
1	Diethylcarbonate (0.5 M)	**SmL** (1 mM)	DIPEA	46
2	$NaHCO_3$ (0.5 M)	**SmL** (1 mM)	DIPEA	78
3	$KHCO_3$ (0.5 M)	**SmL** (1 mM)	DIPEA	68.7
4	Na_2CO_3 (0.5 M)	**SmL** (1 mM)	DIPEA	11
5	K_2CO_3 (0.5 M)	**SmL** (1 mM)	DIPEA	50
6	$CaCO_3$ (0.5 M)	**SmL** (1 mM)	DIPEA	12

[a] Reactions were performed in a solution of MeCN:DIPEA (4:1) containing **SmL** and H_2O (50% v/v) under blue LED irradiation for 4 days.

Table S7. Reactions with different carbonates as CO_2 source.[a]

No.	CO_2 source	Catalyst (conc.)	Sacrificial donor	$\mu moles_{CO}$
1[b]	$NaHCO_3$ (0.5 M)	**SmL** (1 mM)	DIPEA (0.5 mL)	64
2[c]	$NaHCO_3$ (0.5 M)	**SmL** (1 mM)	DIPEA (0.5 mL)	59

[a] Reactions were performed in a solution of MeCN:DIPEA (4:1) containing the catalyst and H_2O (20% v/v) under blue LED irradiation for 4 days; [b] Reaction was carried out with an Ar-purged solution of $NaH^{13}CO_3$; [c] reaction was carried out with a $^{13}CO_2$-purged solution of $NaH^{13}CO_3$.

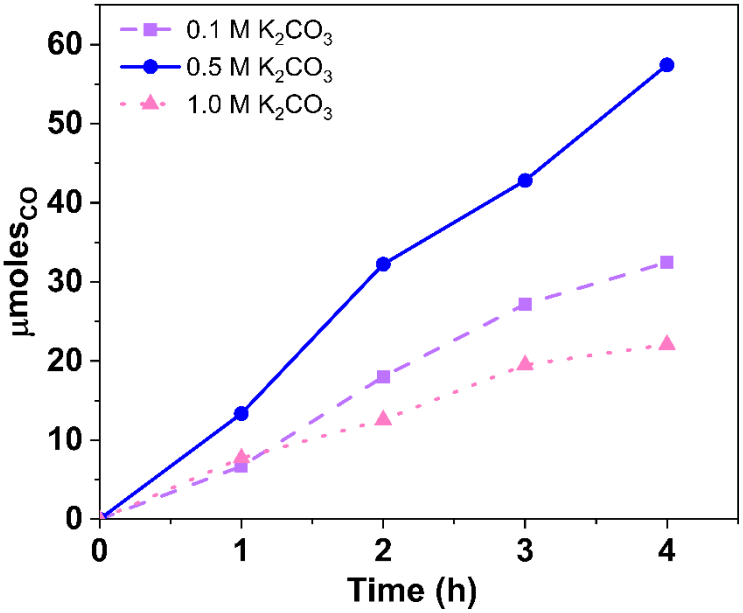

Figure S14. Comparison of the reactivities of reaction mixtures containing different concentrations of K_2CO_3, and **SmL** (100 µM) in MeCN:H_2O (1:1), DIPEA (20%v/v) upon irradiation with blue LED.

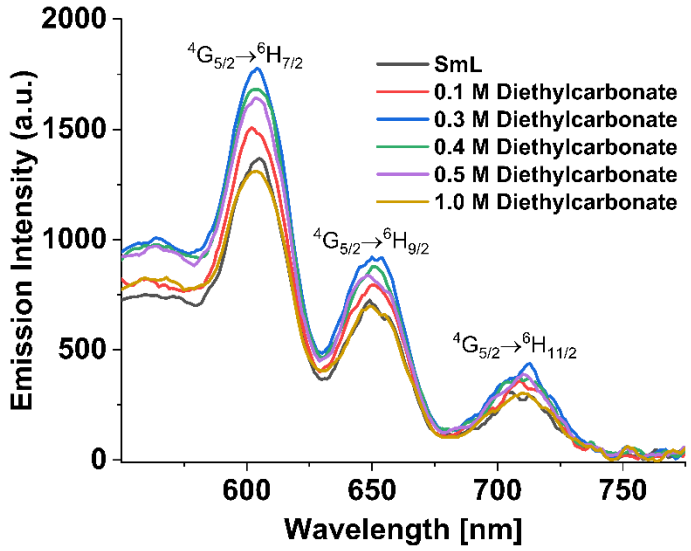

Figure S15. Time-resolved emission of **SmL** (black) in the presence of different concentrations of diethylcarbonate; λ_{ex} = 339 nm, delay time = 0.5 µs.

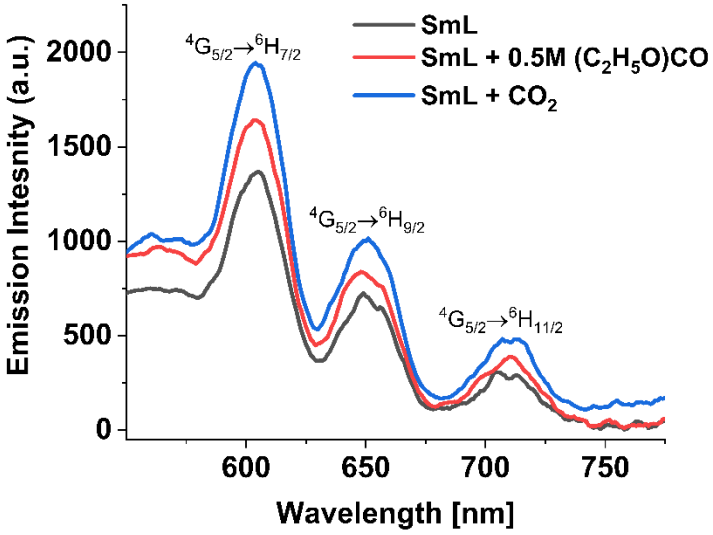

Figure S16. Time-resolved emission of **SmL** (black), SmL with CO2 (blue) and SmL with 0.5 M diethylcarbonate; λ_{ex} = 339 nm, delay time = 0.5 µs.

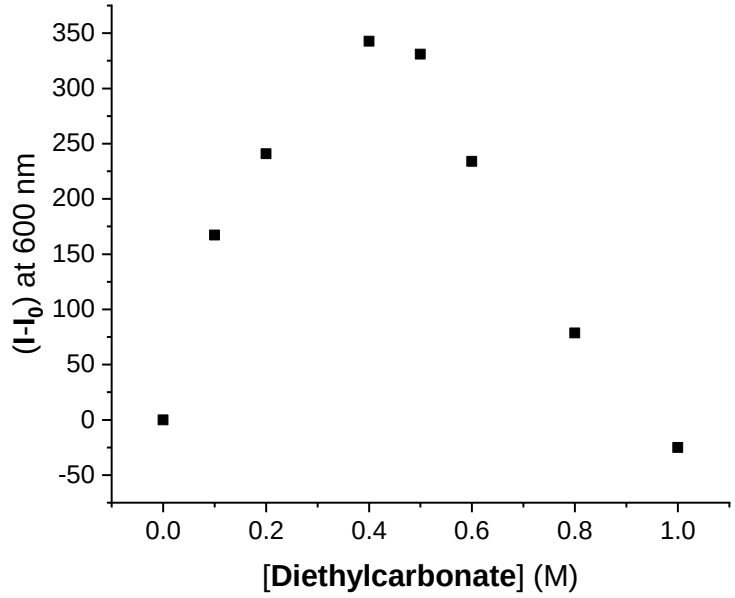

Figure S17. Change in Sm(III) luminescence intensity ($I–I_0$) at λ_{em} = 600 nm as a function of diethylcarbonate concentration, λ_{ex} = 339 nm.

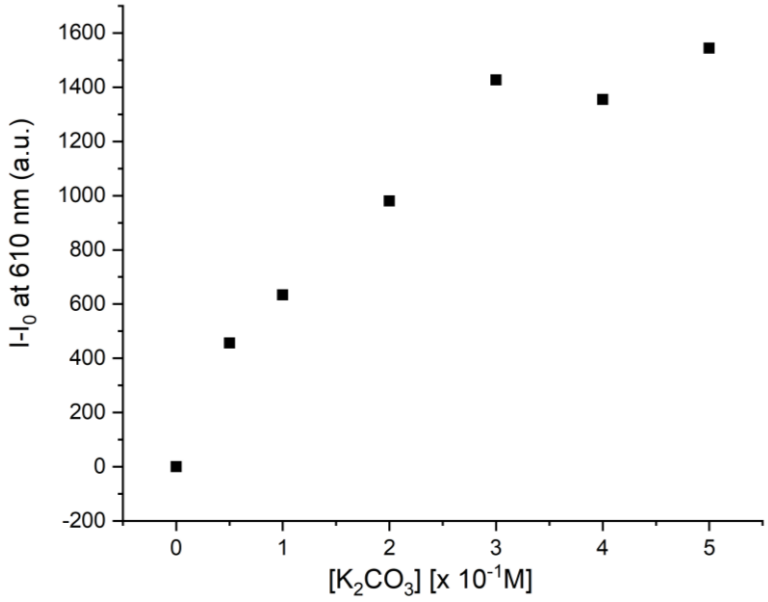

Figure S18. Change in Eu(III) luminescence intensity ($I–I_0$) at λ_{em} = 610 nm as a function of K_2CO_3 concentration, λ_{ex} = 339 nm.

Probing the role of Sm(II) in CO_2RR and carbonate reduction reactions

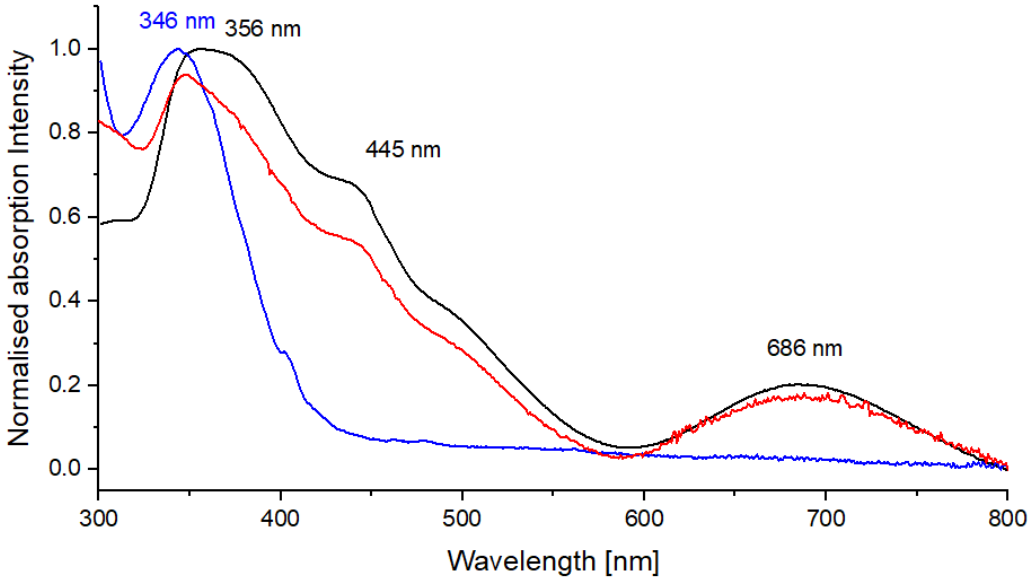

Figure S19. Absorption spectra in MeCN of SmI_2 (black), SmI_2 and diethyl carbonate (1:1) (blue), and SmI_2 solution purged with CO_2 (red); [SmI_2] = 250 μM. Numbers indicate the local maxima.

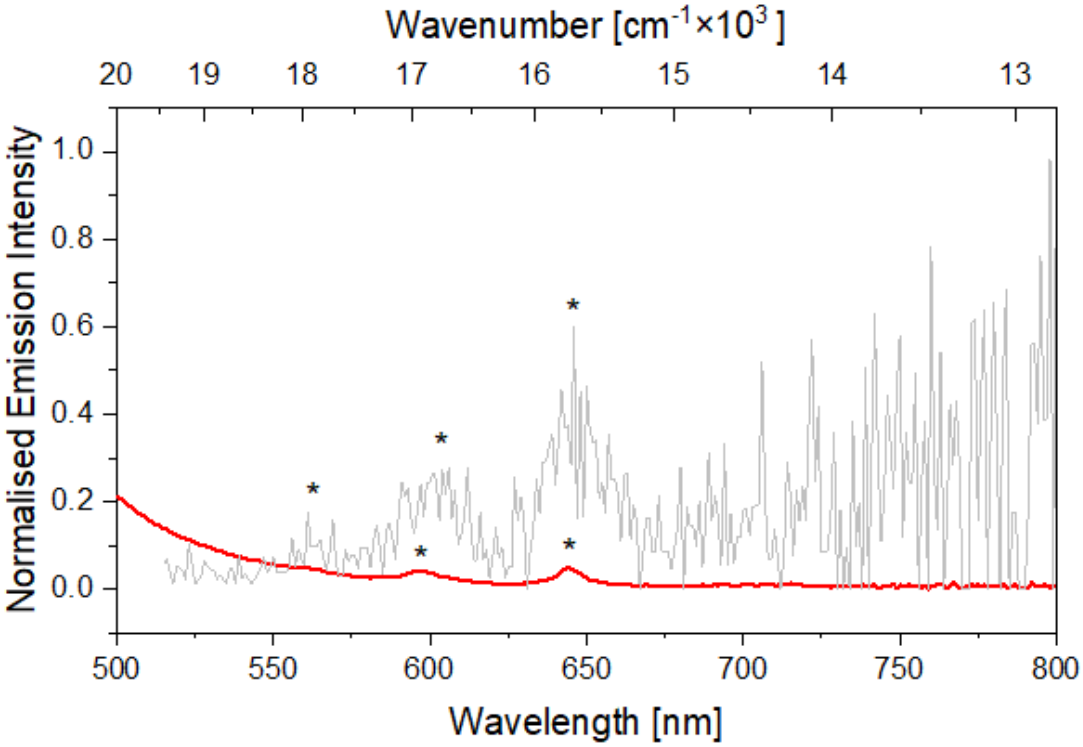

Figure S20. Normalised steady-state (red) and time-resolved (0.05 ms time delay, grey) emission spectra of a SmI_2 solution saturated with CO_2 in MeCN; [SmI_2] = 250 μM, λ_{ex} = 360 nm. Peaks marked with * are due to Sm(III) emission.

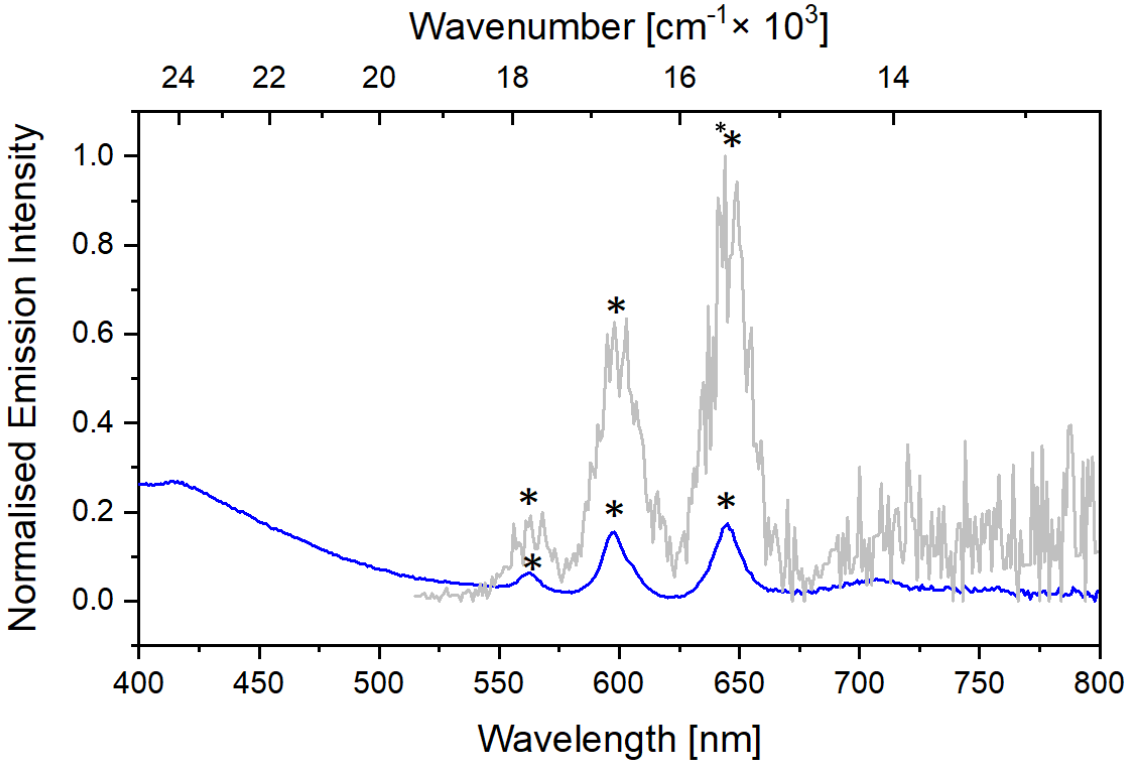

Figure S21. Normalised steady-state (blue) and time-resolved (0.05 ms time delay, grey) emission spectra of a SmI_2 and diethylcarbonate (1:1) in MeCN; [SmI_2] = 250 µM, λ_{ex} = 346 nm. Peaks marked with * are due to Sm(III) emission.

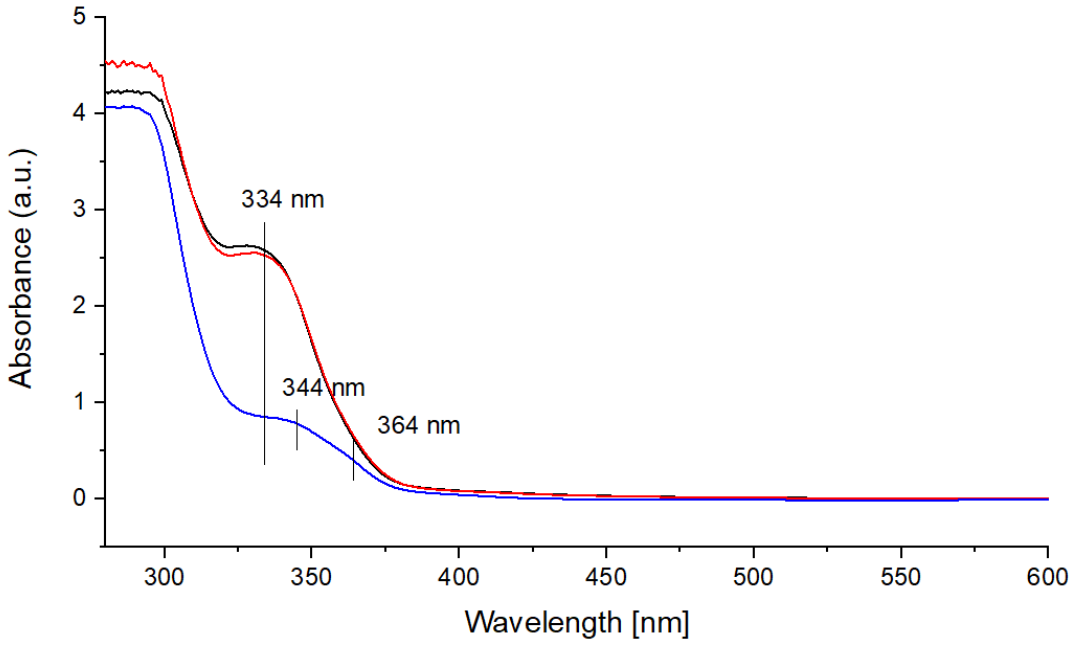

Figure S22. Absorption spectra of a solution of **SmL** (black), **SmL** purged with CO_2 (red), and **SmL** purged with CO_2 after irradiation for 30 min by blue LED (blue); [**SmL**] = 100 µM, in MeCN: 20% H_2O. Numbers indicate the local maxima.

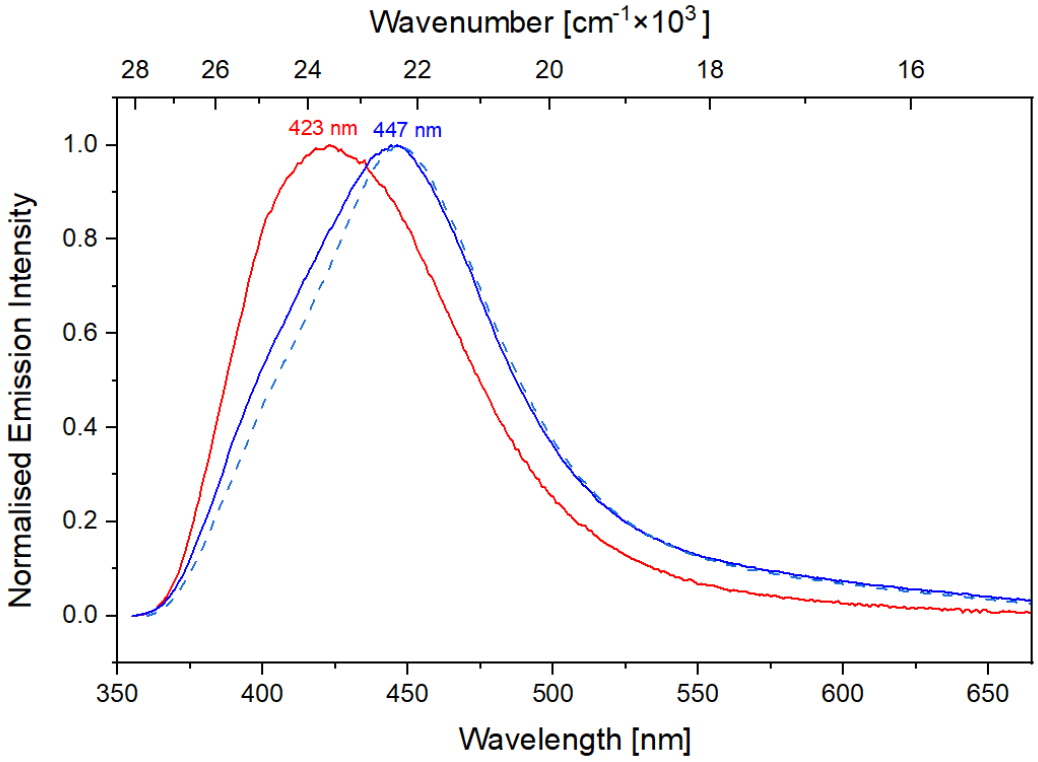

Figure S23. Normalised steady-state emission spectra of a solution of **SmL** purged with CO_2 before (red, λ_{ex} = 340 nm) and after irradiation for 30 min with blue LED (blue, λ_{ex} = 340 nm; blue dotted line, λ_{ex} = 345 nm); [**SmL**] = 100 μM, in MeCN: 20% H_2O. Numbers indicate local maxima.

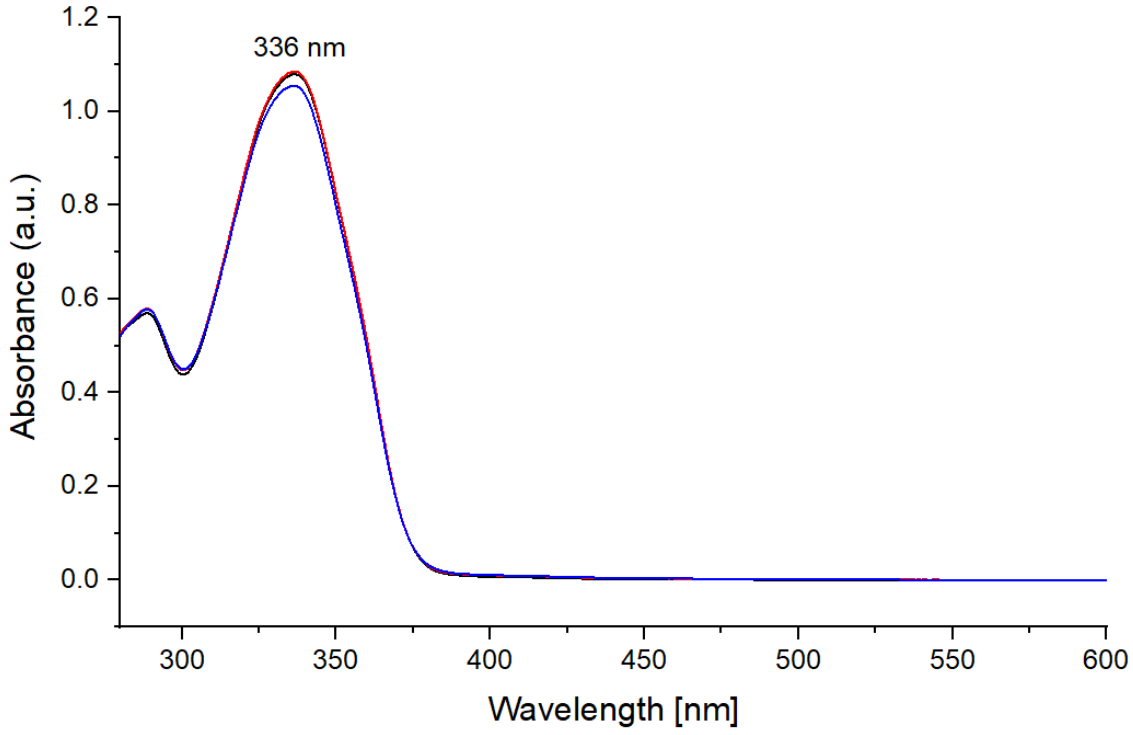

Figure S24. Absorption spectra of **SmL** (black), **SmL** solution purged with CO_2 (red), and **SmL** solution purged with CO_2 after irradiation for 30 min with blue LED (blue); [**SmL**] = 100 μM in MeCN: 20%

H_2O: 20% DIPEA. Numbers indicate local maxima. *Results show that the catalyst is stable during 30 min of irradiation.*

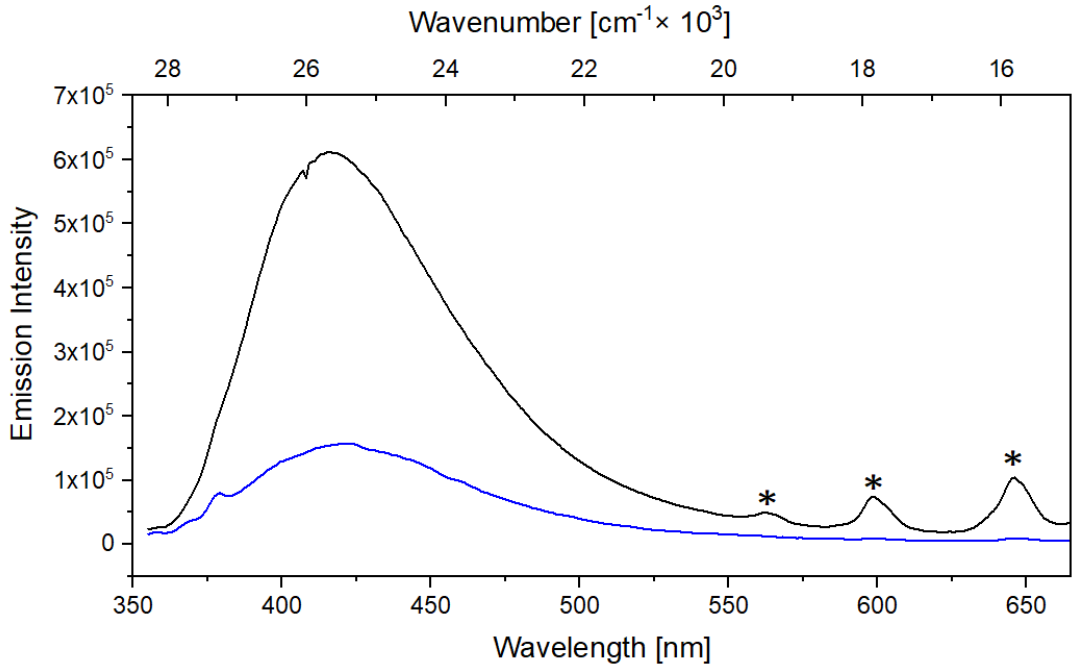

Figure S25. Steady-state emission spectra of a solution of **SmL** (black, λ_{ex} = 340 nm) and of a **SmL** solution purged with CO_2 after irradiation for 30 min with blue LED (blue, λ_{ex} = 340 nm); [**SmL**] = MeCN:20% DMF:0.25% DIPEA. Numbers indicate local maxima. Peaks marked with * are due to Sm(III) emission.

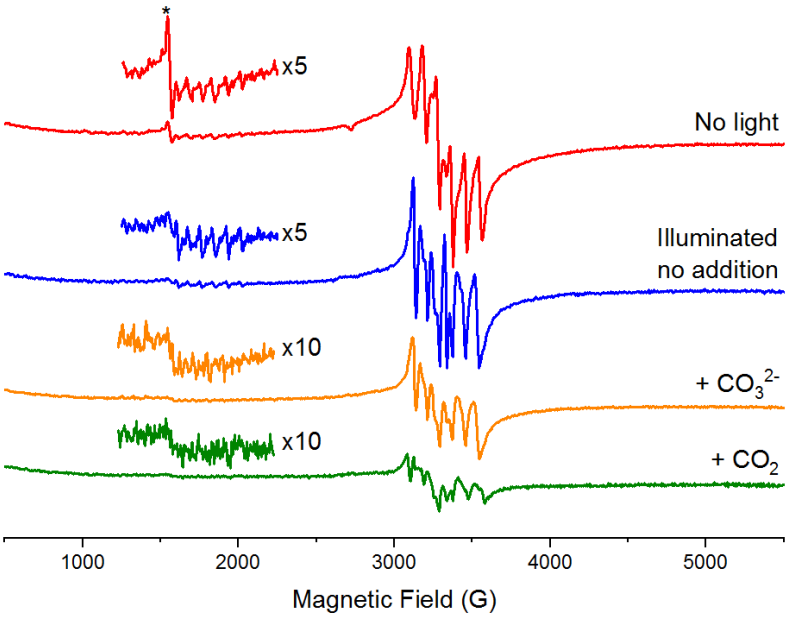

Figure S26. EPR spectra (g ~ 2 region) at 10 K of Sm(III)**L** before (red) and after (blue) illumination, and after addition of CO_3^{2-} (orange) or CO_2 (green). The EPR signal from a sample of SmI_2 with added

CO_2, magnified by a factor of 3, is also shown for reference. The vertical lines show the different width of the EPR signals from the different species. EPR parameters: microwave power, 200 µW, modulation amplitude 10 G.

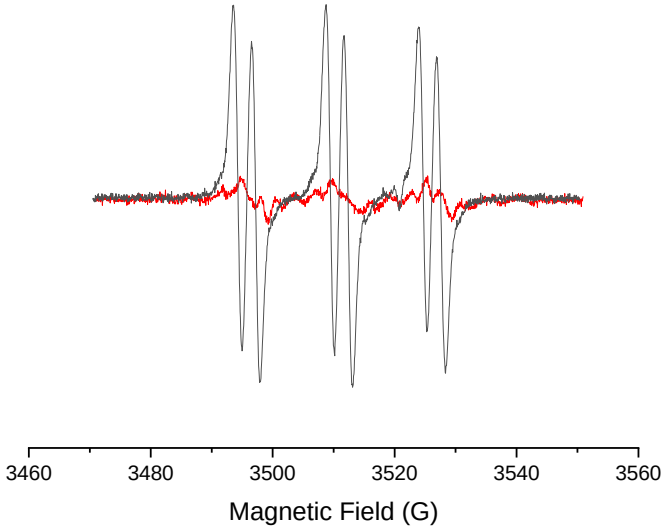

Figure S27. Room temperature EPR spectra of a solution of **SmL** (1 µM) in $^{13}CO_2$-saturated MeCN:DIPEA (4:1), H_2O (20%) and N-tert-butyl-α-phenylnitrone (PBN) (1 mM) (black), and **SmL** (1 µM) in Ar-saturated MeCN:DIPEA (4:1), H_2O (20%) and N-tert-butyl-α-phenylnitrone (PBN) (1 mM) (red) collected after 16 h irradiation with blue LED showing the formation of a radical, EPR parameters: microwave power, 2 mW, modulation amplitude, 1 G. The magnetic field values of the black spectrum have been adjusted to account for fluctuations in the microwave frequency.

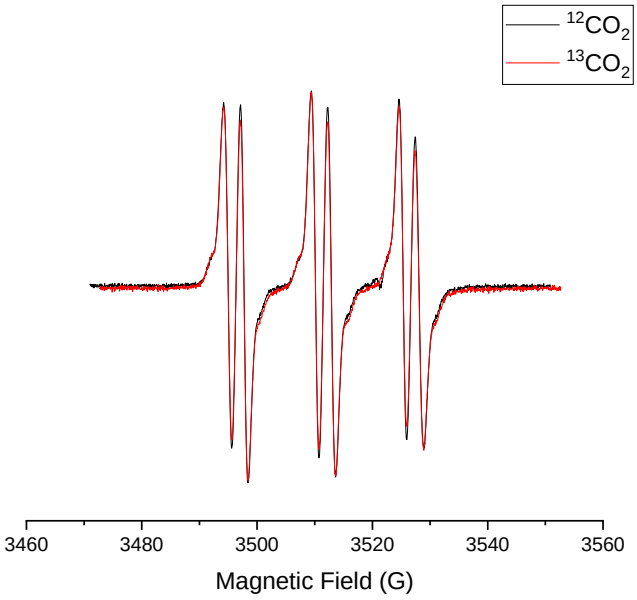

Figure S28. Room temperature EPR spectra of a solution of **SmL** (1 μM) in CO_2-saturated MeCN:DIPEA (4:1), H_2O (20%) and N-tert-butyl-α-phenylnitrone (PBN) (1 mM) (black), and **SmL** (1 μM) in $^{13}CO_2$-saturated MeCN:DIPEA (4:1), H_2O (20%) and N-tert-butyl-α-phenylnitrone (PBN) (1 mM) (red) collected after 16 h irradiation with blue LED showing the formation of a radical, EPR parameters: microwave power, 2 mW, modulation amplitude, 1 G. The magnetic field values of the red spectrum have been adjusted to account for fluctuations in the microwave frequency.

Concentration dependence of formic acid formation

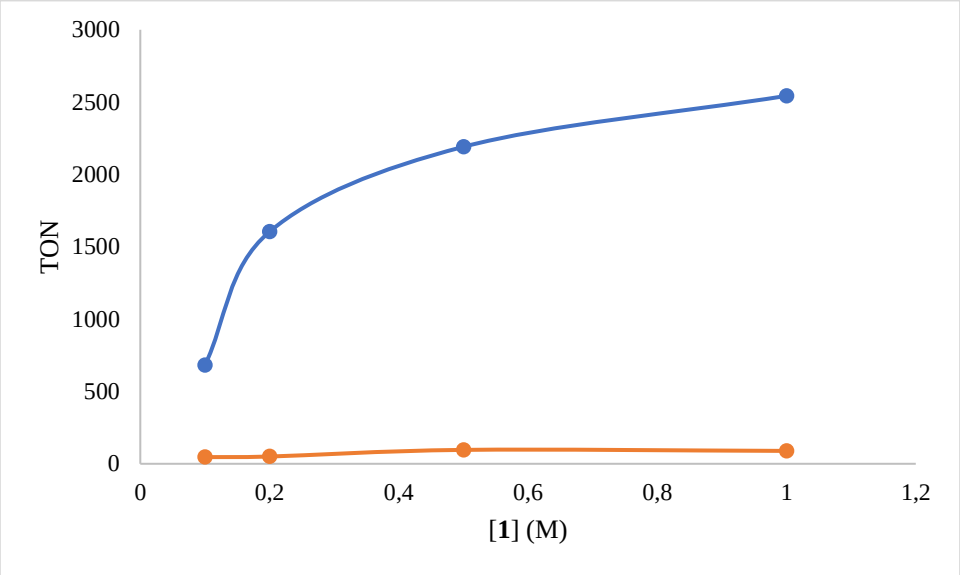

Figure S29. Concentration dependence of $TON_{formate}$ (blue) and TON_{CO} (orange) shown for reactions containing 0.1 M, 0.2 M, 0.5 M or 1 M BIH, using **SmL** (100 µM) catalyst in CO_2-saturated solutions of MeCN:DIPEA (4:1) under blue LED irradiation.

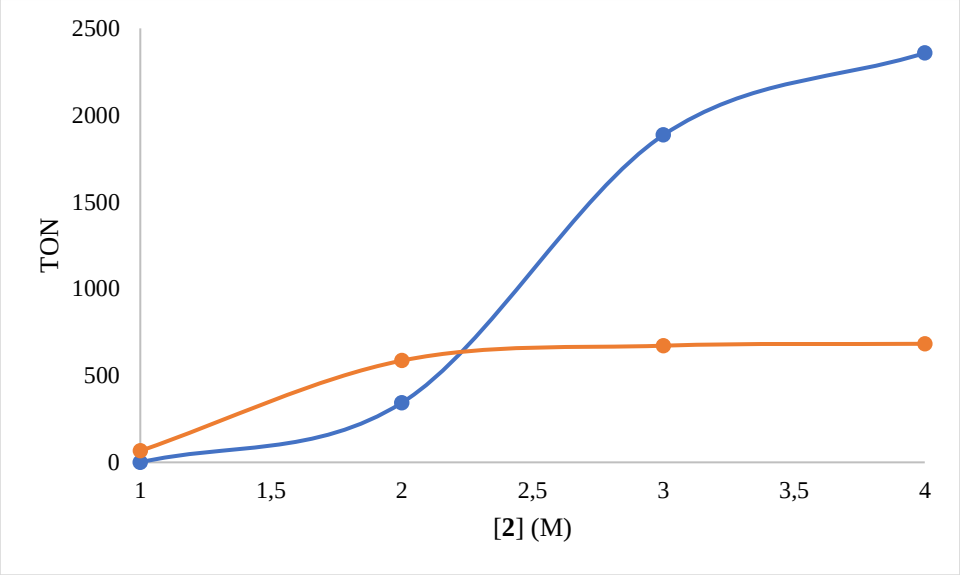

Figure S30. Concentration dependence of $TON_{formate}$ (blue) and TON_{CO} (orange) shown for reactions containing 0.1 M, 0.2 M, 0.5 M or 1 M of **2**, using **SmL** (100 µM) catalyst in CO_2-saturated solutions of MeCN:DIPEA (4:1) under blue LED irradiation.

The role of BI(OH)H

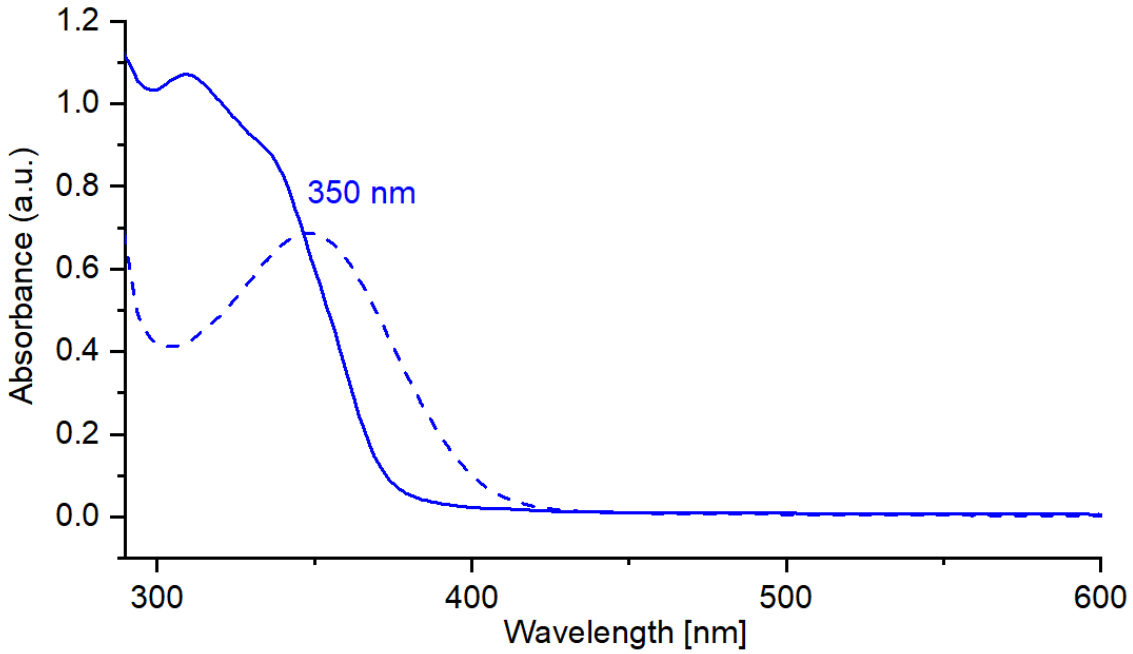

Figure S31. Absorption spectrum of a reaction mixture containing BI(OH)H, DIPEA, and **SmL** before (blue) and after 35 mins of irradiation (blue dashed) with blue LED. [**SmL**] = 50 μM = [BI(OH)H] = [DIPEA], in MeCN containing 20% H_2O.

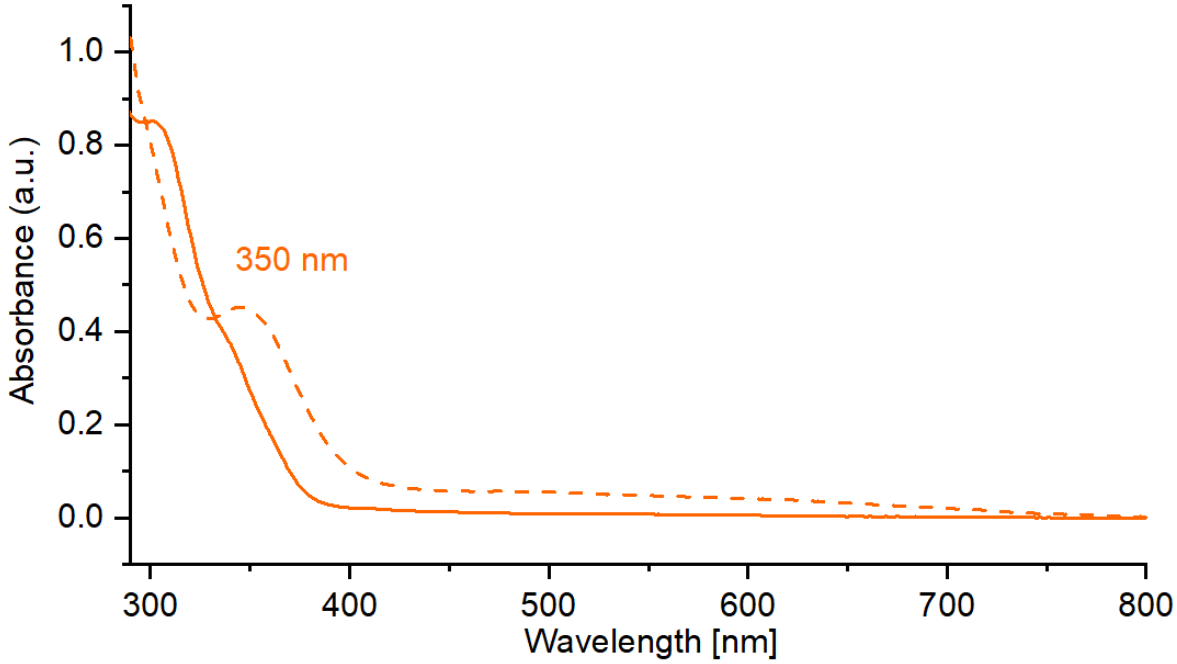

Figure S32. Absorption spectrum of a reaction mixture containing BI(OH)H, DIPEA, **SmL** and CO_2 before (orange) irradiation after 35 mins of irradiation (orange dashed line) with blue LED. [**SmL**] = 50 μM = [BI(OH)H] = [DIPEA] in MeCN containing 20% H_2O]. Sm(III) emission was not observed upon direct excitation at λ_{ex} = 401 nm, or in time-resolved mode either.

Quantification of [HCO_3^-] before and after the reaction

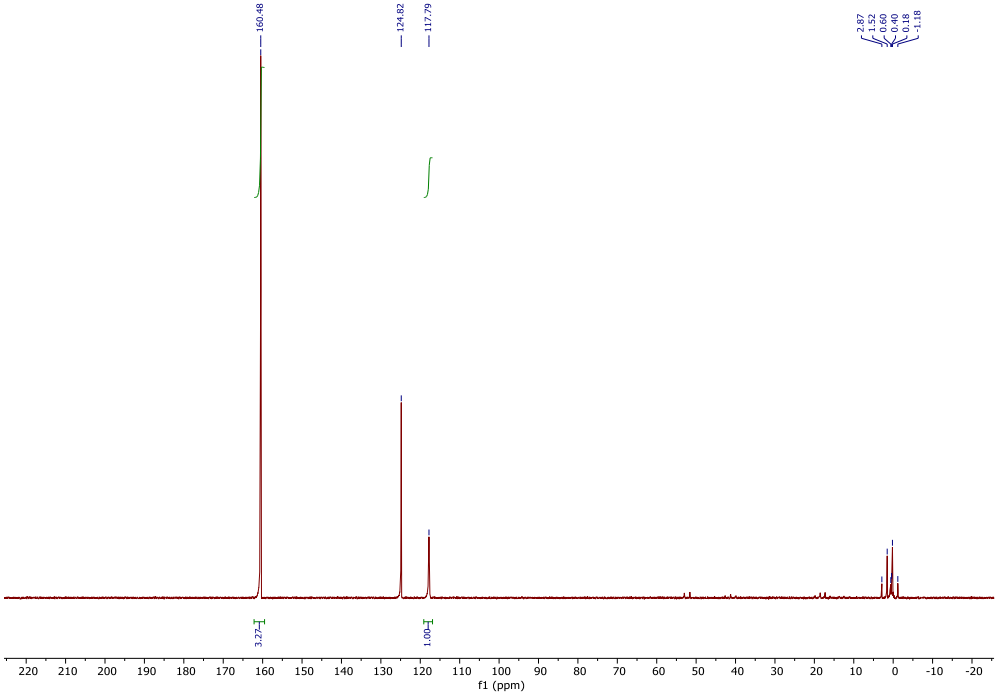

Figure S33. ^{13}C NMR spectrum of a CO_2-purged solution of **SmL** (1 μM) in MeCN:DIPEA (4:1) containing water (20% v/v) before irradiation.

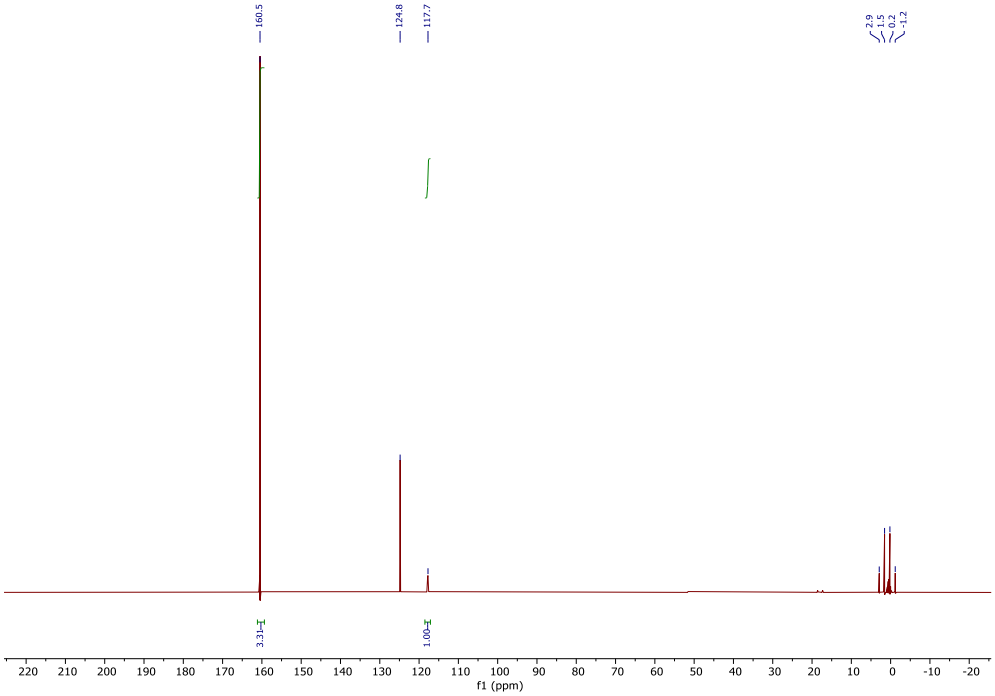

Figure S34. ^{13}C NMR of a CO_2-purged solution of **SmL** (1 μM) in MeCN:DIPEA (4:1), water (20% v/v) after 16 h irradiation with blue LED, showing that the [HCO_3^-] (δ = 160.5 ppm) is similar to before reaction within experimental error.

^{13}C-labelling studies

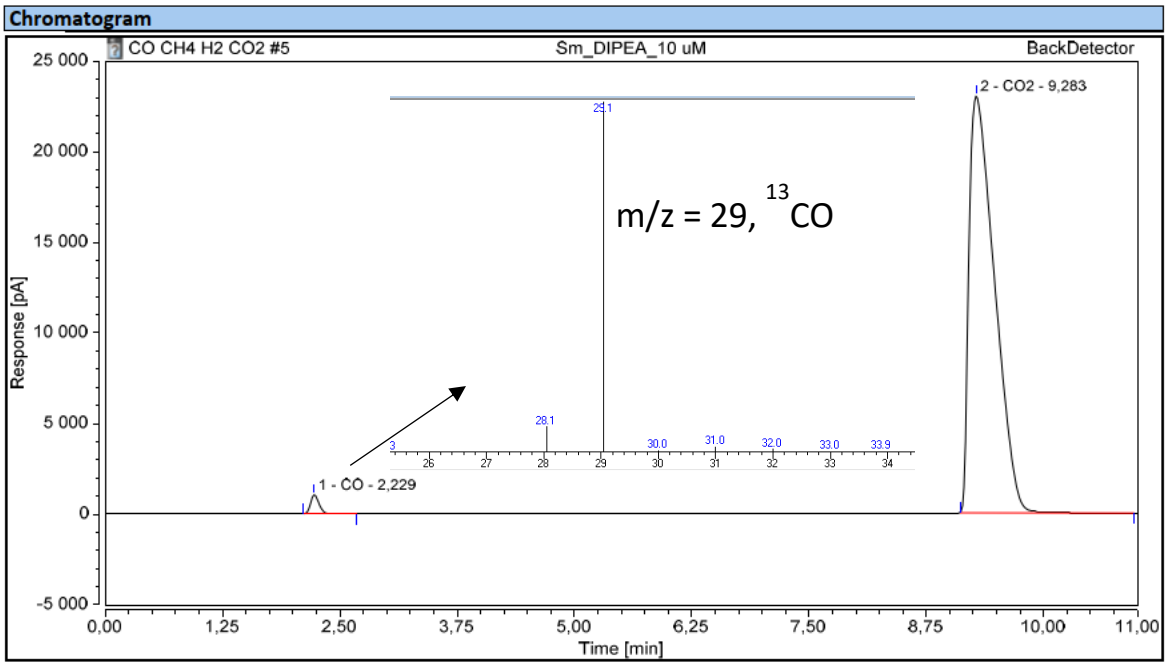

Figure S35. GC-MS trace of the reaction mixture of $^{13}CO_2$ with **SmL** (10 µM), water (20%), MeCN:DIPEA (4:1) under blue LED irradiation for 16 h, showing the formation of ^{13}CO as the product.

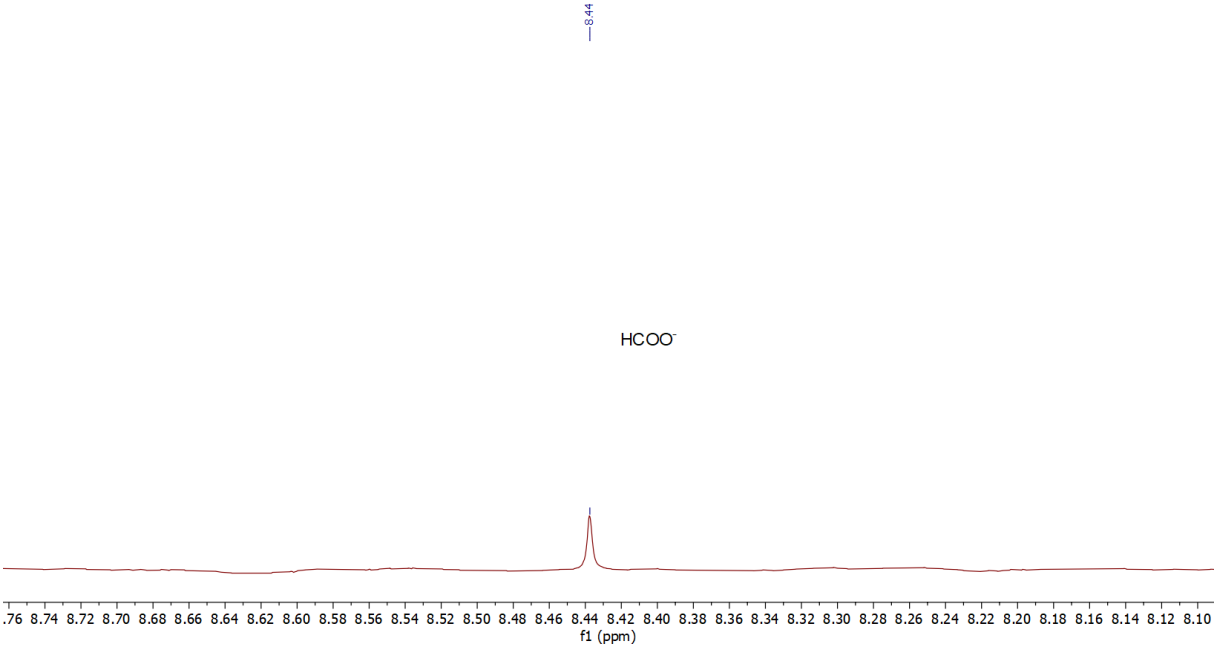

Figure S36. ^{1}H NMR spectrum of the reaction mixture of a CO_2-purged solution of MeCN:DIPEA (4:1) containing **SmL** (100 µM) and water (20%v/v) after 16 h of irradiation with blue LED.

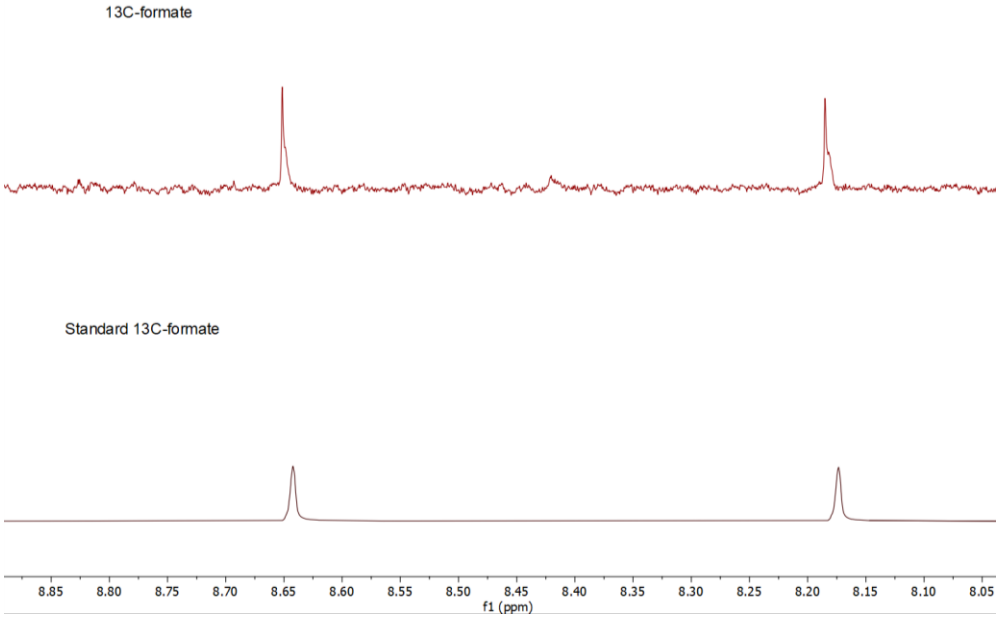

Figure S37. ^{1}H NMR spectrum for the reaction mixture of a $^{13}CO_2$-purged solution of MeCN:DIPEA (4:1) containing **SmL** (100 µM) and water (20%v/v) after 16 h of irradiation with blue LED, showing the presence of $H^{13}COO^-$ (above) and its comparison with standard ^{13}C-formate (below).

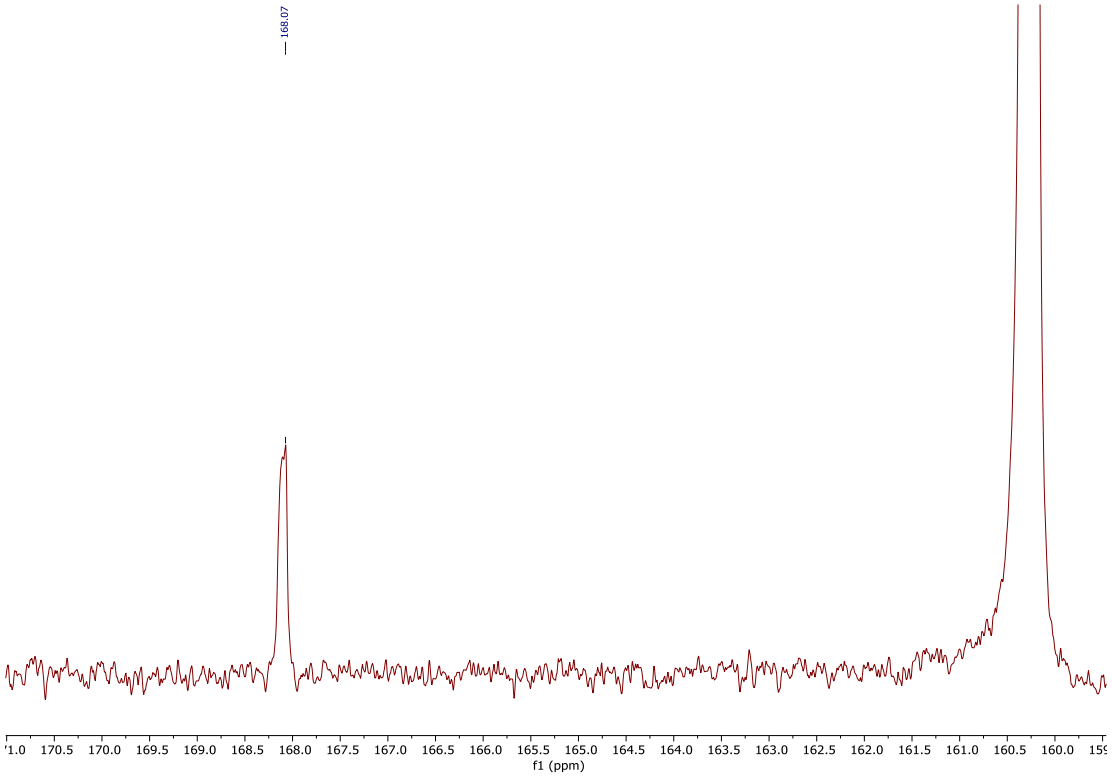

Figure S38. ^{13}C NMR spectrum of the reaction mixture of a $^{13}CO_2$-saturated solution of MeCN:DIPEA (4:1) containing **SmL** (100 µM) and water (20%v/v) after 16 h of irradiation with blue LED, showing presence of $H^{13}COO^-$.

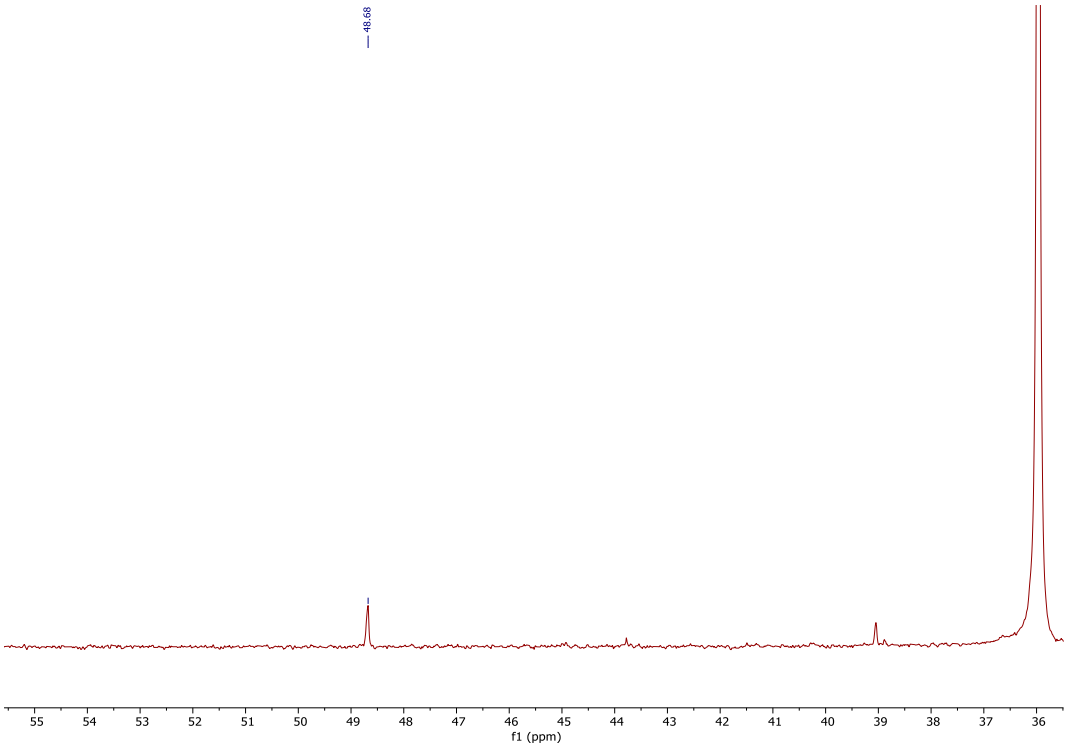

Figure S39. ^{13}C NMR spectrum for the reaction mixture of a CO-purged solution of DMF:H_2O (4:1) containing **SmL** (100 µM), **2** (1 M) showing the presence of CH_3OH.

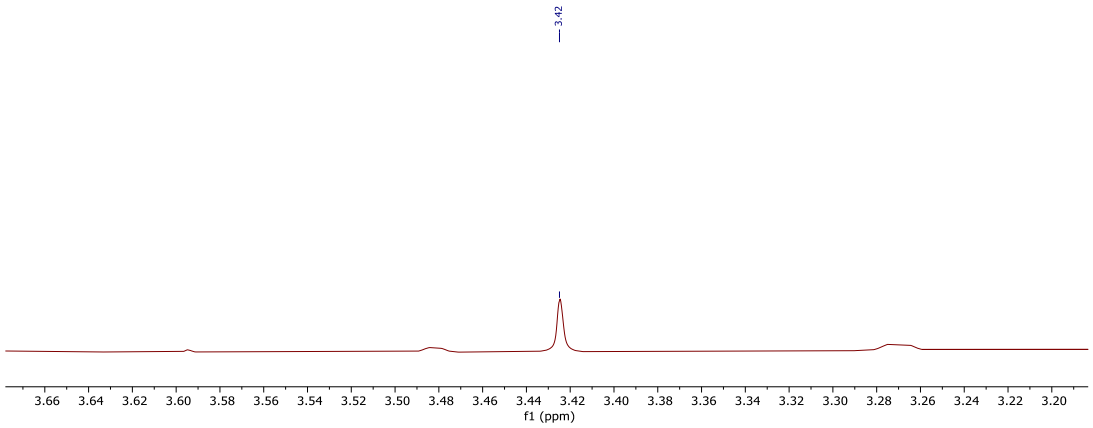

Figure S40. ^{1}H NMR spectrum for the reaction mixture of a CO-purged solution of DMF:H_2O (4:1) containing **SmL** (100 µM), **2** (1 M) showing the presence of CH_3OH.

Effect of proton donors

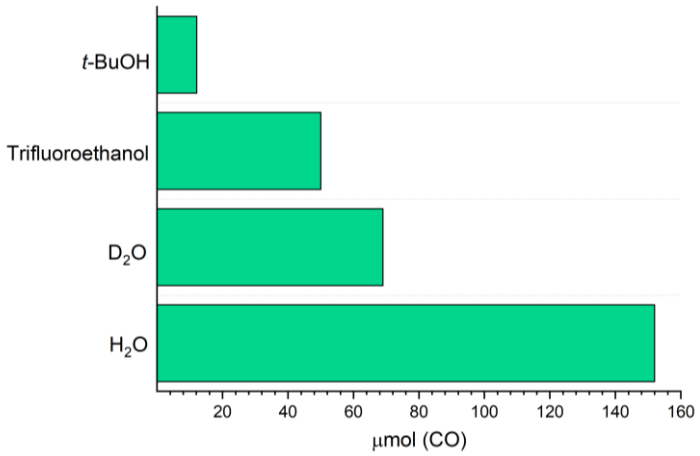

Figure S41. Comparison of the reactivity of **SmL** (1 µM) in CO_2-saturated MeCN:DIPEA (4:1) solutions after 16 h irradiation in the presence of different proton sources.

Table S8. Eu(III) luminescence lifetimes of EuL in DMF.

EuL	**τ_{Eu} (ms)** [a]	**goodness of fit (R^2)**
in DMF	0.57	0.80
20% ^{t}BuOH in DMF	t_1 = 0.11 (monoexponential) t_2 = 0.45 (biexponential; A_1 = 811, A_2 = 64)	0.908 (monoexponential) 0.947 (biexponential)
in H_2O	t_1 = 0.14 (monoexponential) t_2 = 1.5 (biexponential; A_1 = 47.79; A_2 = 2.39)	0.128 (monoexponential) 0.133 (biexponential)
in D_2O	2.63	0.93

[a] λ_{ex} = 339 nm, λ_{em} = 610 nm. Initial delay: 0.05, delay increment: 0.01, total time monitored: 10 ms.

Table S9. Comparison of SmL with the best photocatalysts for CO_2RR reported in literature.[a]

Entry	Sensitizer	Catalyst	Sacrificial donor	TON_{CO} (% selectivity)	TON_{HCOOH} (% selectivity)
1[b]	-	**SmL**	**DIPEA**	**377530 (>99)**	-
2[b]	-	**SmL**	**BI(OH)H, DIPEA**	-	**2239 (>99)**
3[5]	Cu-purpurin	FeTDHPP	BIH	7650 (95)	-
4[6]	-	Metal-organic-zyme	BIH	24740 (98)	-
5[7]	-	Ir_1/A-aUiO	H_2O:IPA (4:1)	0	692 (99)
6[8]	$Ir(ppy)_3$	Ni-NHC	BIH	310000 (90)	-
7[9]	$[Ru(Phen)_3]^{2+}$	$[Co_2(biqpy)]^{4+}$	BIH, PhOH	829 (96)	12 (1.5)
8	$[Ru(Phen)_3]^{2+}$	$[Co_2(biqpy)]^{4+}$	BIH, TEA	386 (96.5)	8 (2)
9[10]	-	Mes-Ir(PCY)$_2$	BIH	470 (18)	2080 (81)

[a] FeTDHPP = Fe-tetrakis(dihydroxyphenyl)porphyrin; Phen = 1,10-phenanthroline; biqpy = 4,4′′′′-(2,7-di-tert-butyl-9,9-dimethyl-9H-xanthene-4,5-diyl) di-2,2′:6′,2′′:6′′,2′′′-quaterpyridine. 1,3-dimethyl-2-phenylbenzimidazoline (BIH); NHC = N-hetercycliccarbene; Mes = 2,4,6-tri-*tert*-butylphenyl; PCY = bicyclohexylphosphine; ppy = 2-phenylpyridine; Metal-organic-zyme = $Hf_{12}(\mu_3\text{-}O)_8(\mu_3\text{-}OH)_8(\mu_2\text{-}OH)_6$(Ir-PS)$_6(TFA)_6$Ir(4,4′-di(4-benzoato)-2,2′-bipyridine)[2-(2,4-difluorophenyl)- 5 (trifluoromethyl)pyridine]$_2^+$; aUiO = NH_2-UiO-66. [b] This work.

^{1}H NMR spectra and GC-MS traces

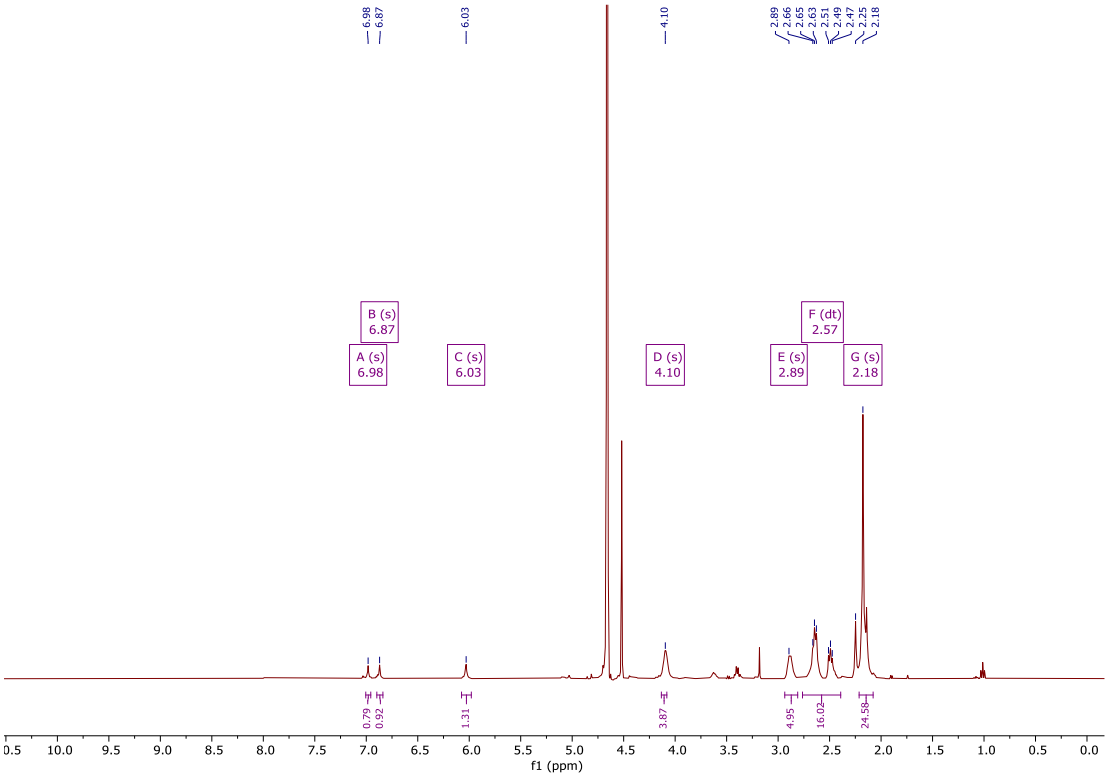

Figure S42. ^{1}H NMR spectrum of $\mathbf{L^{Me}}$ (400 MHz, D_2O).

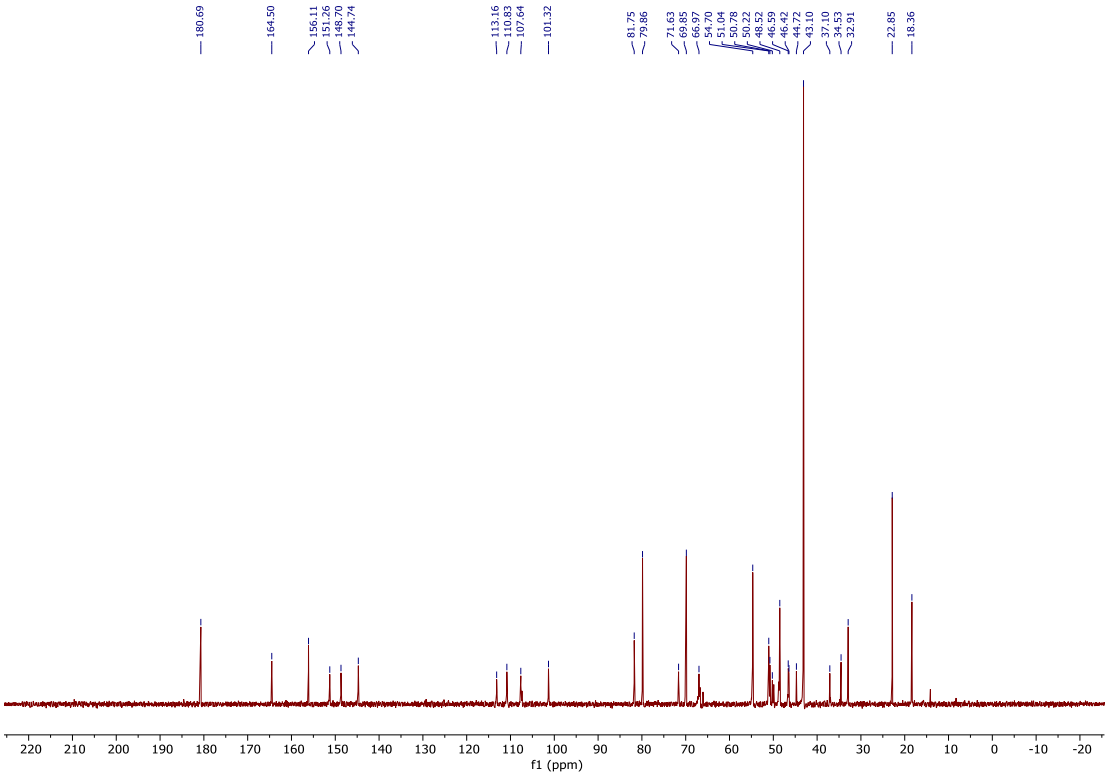

Figure S43. ^{13}C NMR spectrum of $\mathbf{L^{Me}}$ (101 MHz, D_2O).

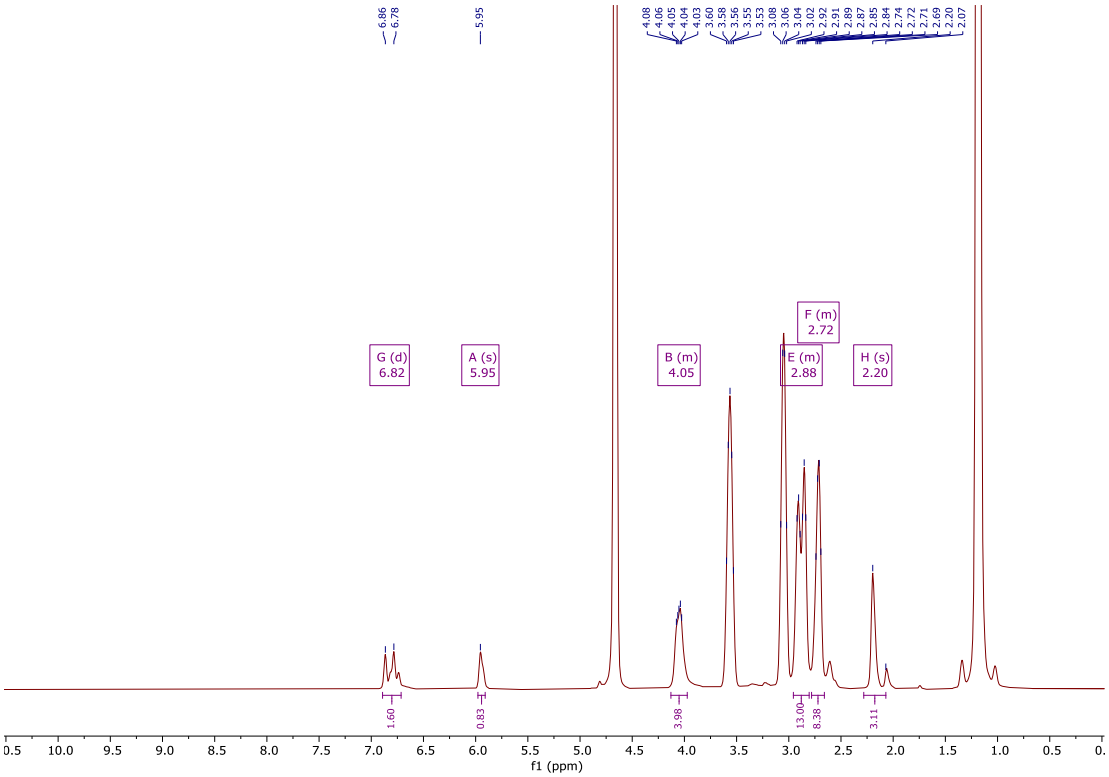

Figure S44. ^{1}H NMR spectrum of ^{13}C-$\mathbf{L^{CO2}}$ (400 MHz, D_2O).

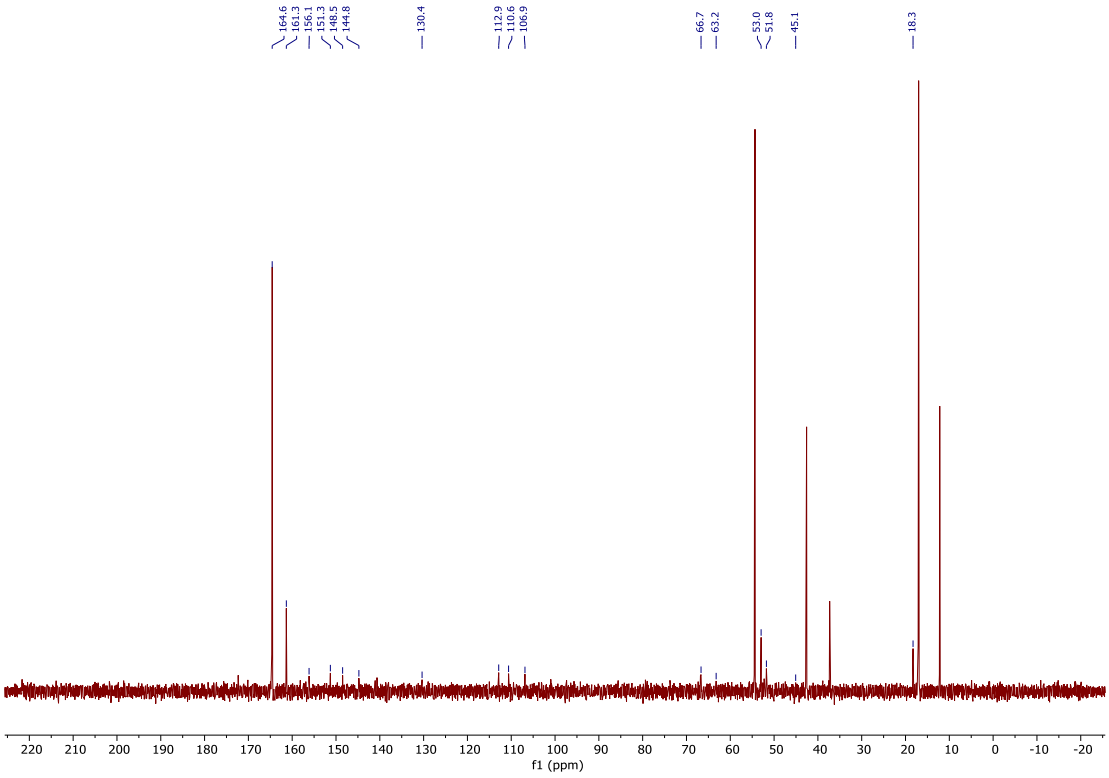

Figure S45. ^{13}C NMR spectrum of ^{13}C-$\mathbf{L^{CO2}}$ (101 MHz, D_2O).

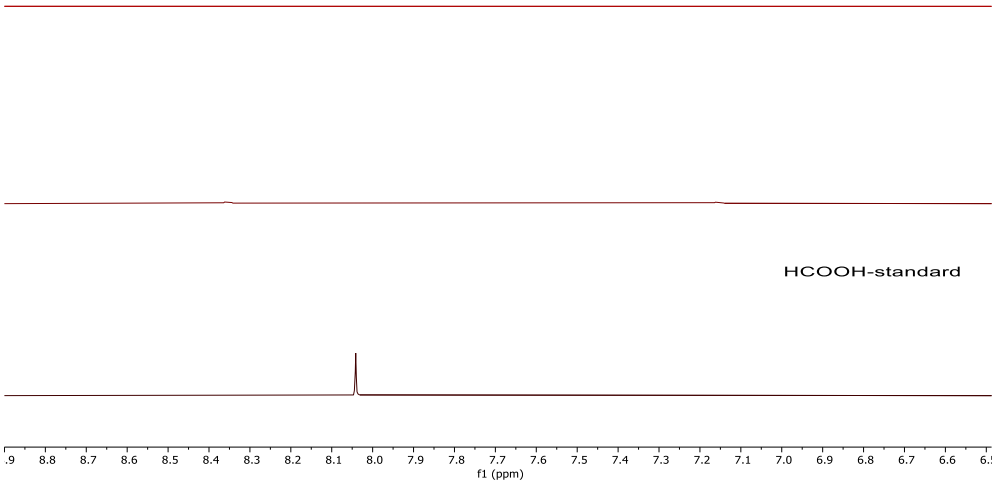

Figure S46. Analysis of liquid products using ^{1}H NMR for the reaction of **SmL** (10 µM) in a CO_2-purged solution of MeCN:DIPEA (4:1) and water (20%) under blue LED irradiation for 16 h. The results show that formate is not formed.

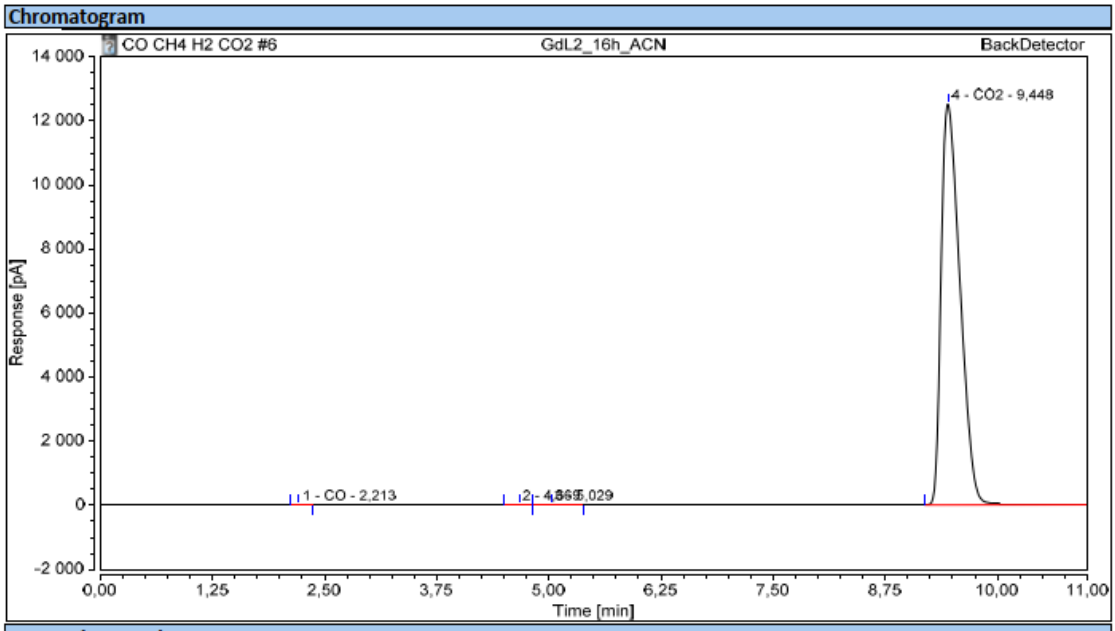

Integration Results

No.	Peak Name	Retention Time min	Area pA*min	Height pA	Relative Area %	Relative Height %	Amount umol
1	CO	2,213	0,192	2,549	0,01	0,02	n.a.
n.a.	CH4	n.a.	n.a.	n.a.	n.a.	n.a.	n.a.
2		4,669	0,024	0,140	0,00	0,00	n.a.
3		5,029	0,043	0,109	0,00	0,00	n.a.
4	CO2	9,448	3041,751	12504,097	99,99	99,98	475,1475
Total:			**3042,011**	**12506,895**	**100,00**	**100,00**	

Figure S47. Analysis of gas phase products using GC-MS for the reaction of **GdL** (10 µM) in a CO_2-purged solution of MeCN:DIPEA (4:1), water (20%) under blue LED irradiation for 16 h.

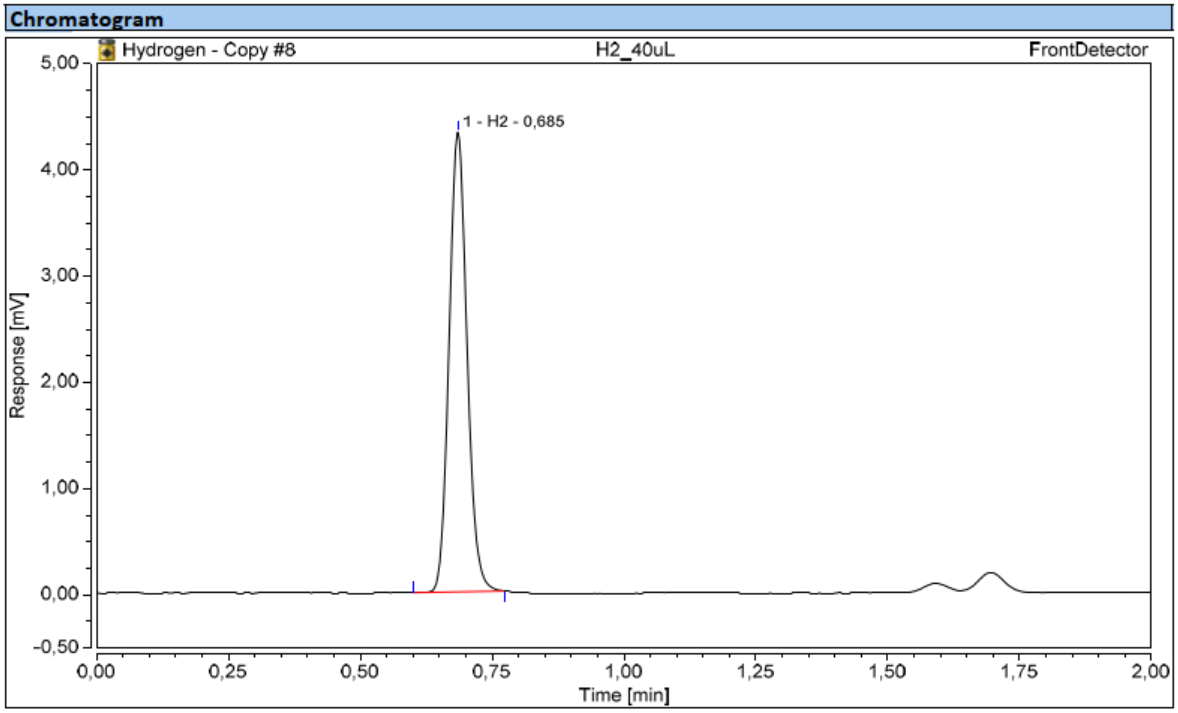

Figure S48. Reference GC trace (front detector) of H_2 after injection of 40 µL of pure H_2 gas.

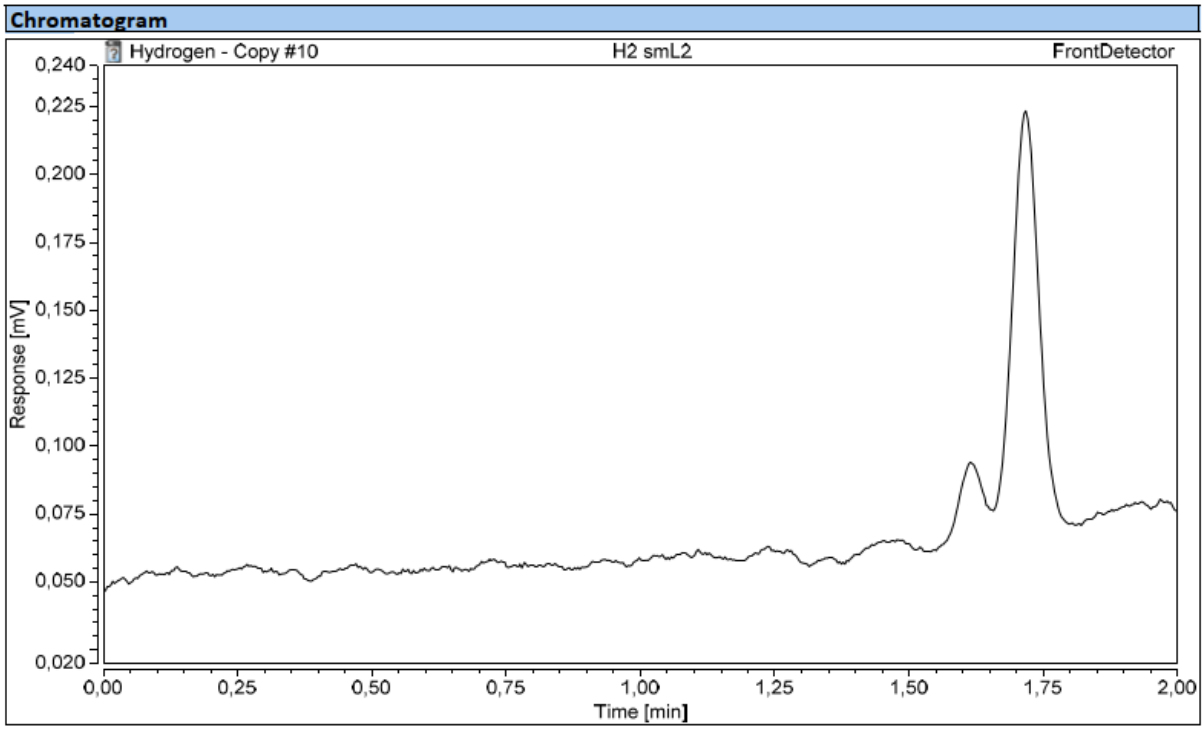

Figure S49. Analysis of gas phase products using GC for the reaction of **SmL** (1 µM) in a CO_2-purged solution of MeCN:DIPEA (4:1), water (20%) under blue LED irradiation for 16 h. *This (front detector) GC trace shows lack of H_2 formation in the reaction.*

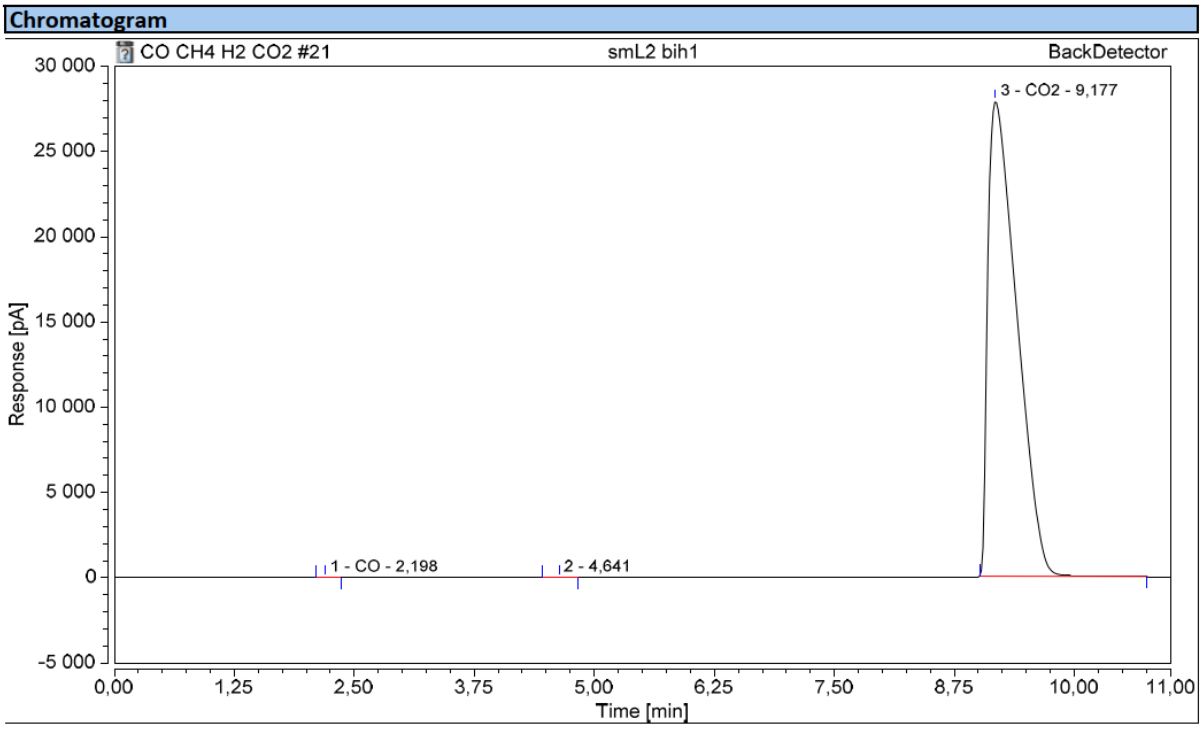

Figure S50. Analysis of gas phase products using GC for the reaction of **SmL** (100 μM), **1** (1 M) in a CO_2-purged solution of MeCN:DIPEA (4:1), water (20%) under blue LED irradiation for 48 h. *This (back-detector) GC trace shows lack of CO formation in the reaction.*

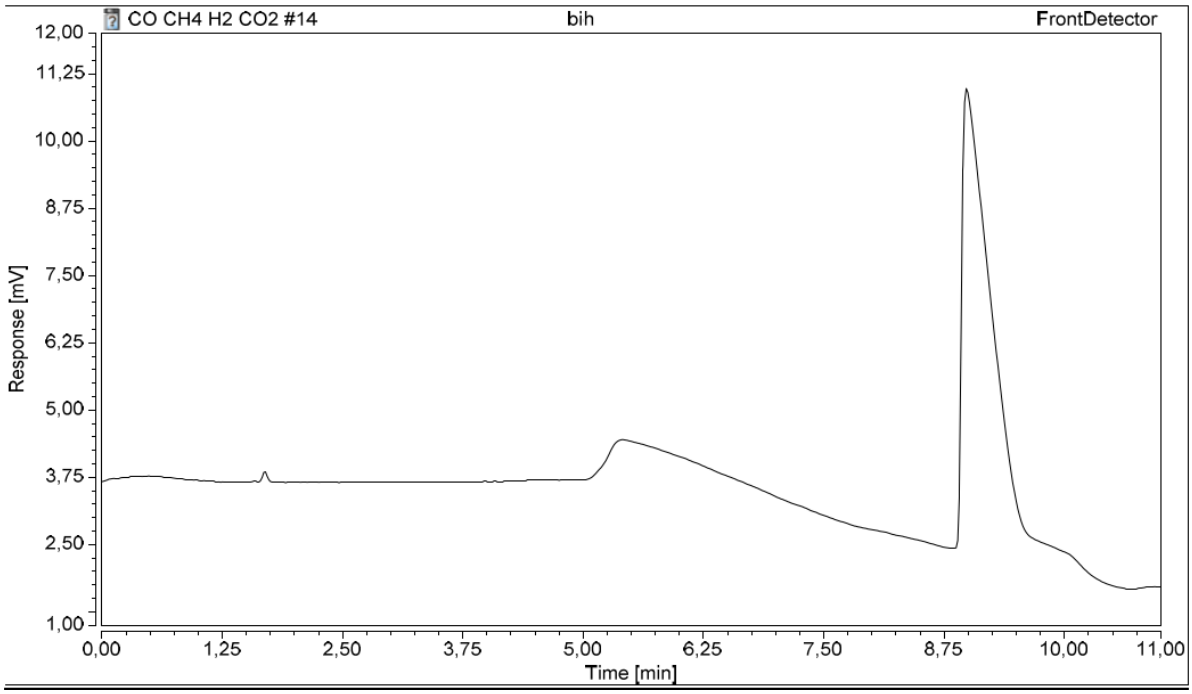

Figure S51. Analysis of gas phase products using GC for the reaction of **SmL** (100 μM), **1** (1 M) in a CO_2-purged solution of MeCN:DIPEA (4:1), water (20%) under blue LED irradiation for 48 h. *This (front-detector) GC trace shows lack of H_2 formation in the reaction.*

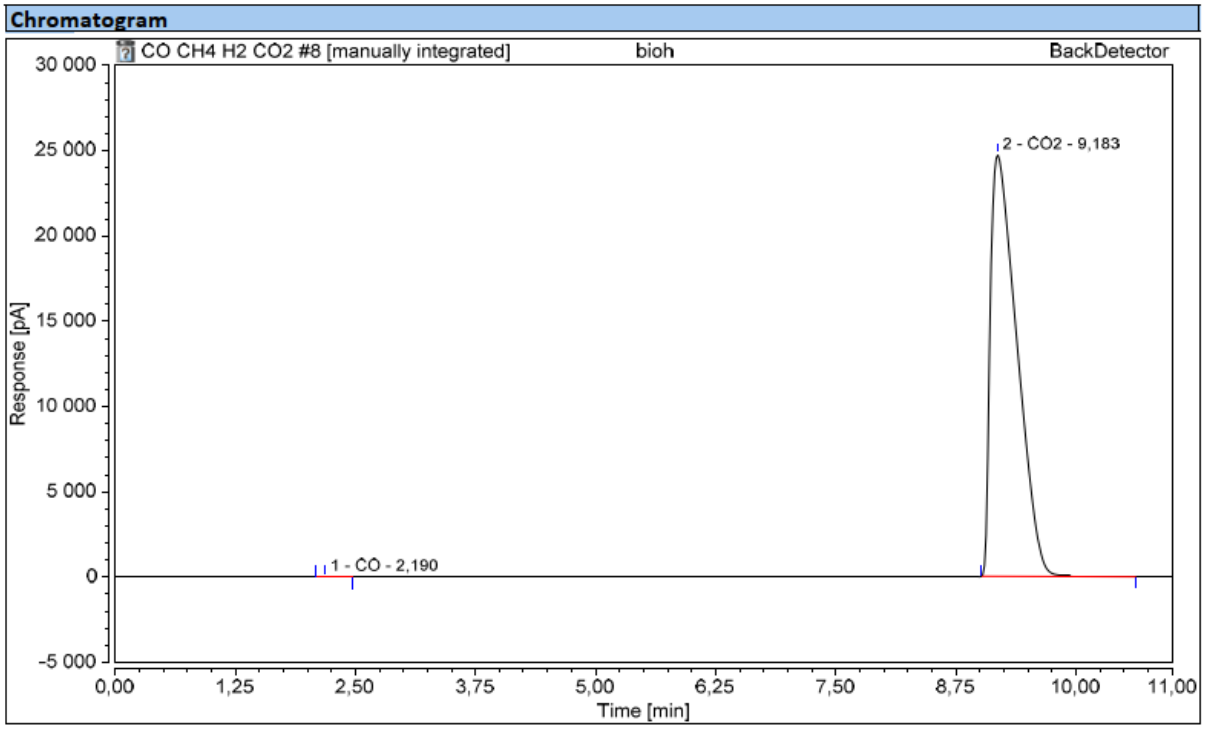

Figure S52. Analysis of gas phase products using GC for the reaction of **SmL** (100 μM), **2** (1 M) in a CO_2-purged solution of MeCN:DIPEA (4:1), water (20%) under blue LED irradiation for 48 h. *This (back-detector) GC trace shows lack of CO formation in the reaction.*

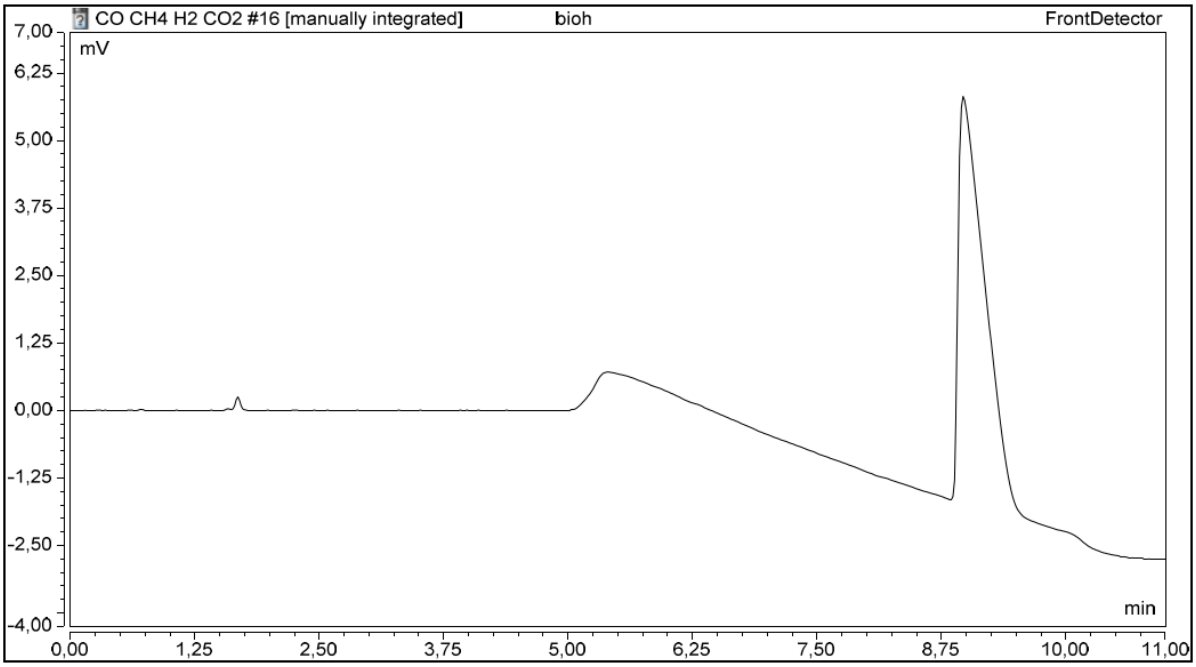

Figure S53. Analysis of gas phase products using GC for the reaction of **SmL** (100 μM), **2** (1 M) in a CO_2-purged solution of MeCN:DIPEA (4:1), water (20%) under blue LED irradiation for 48 h. *This (front-detector) GC trace shows lack of H_2 formation in the reaction.*

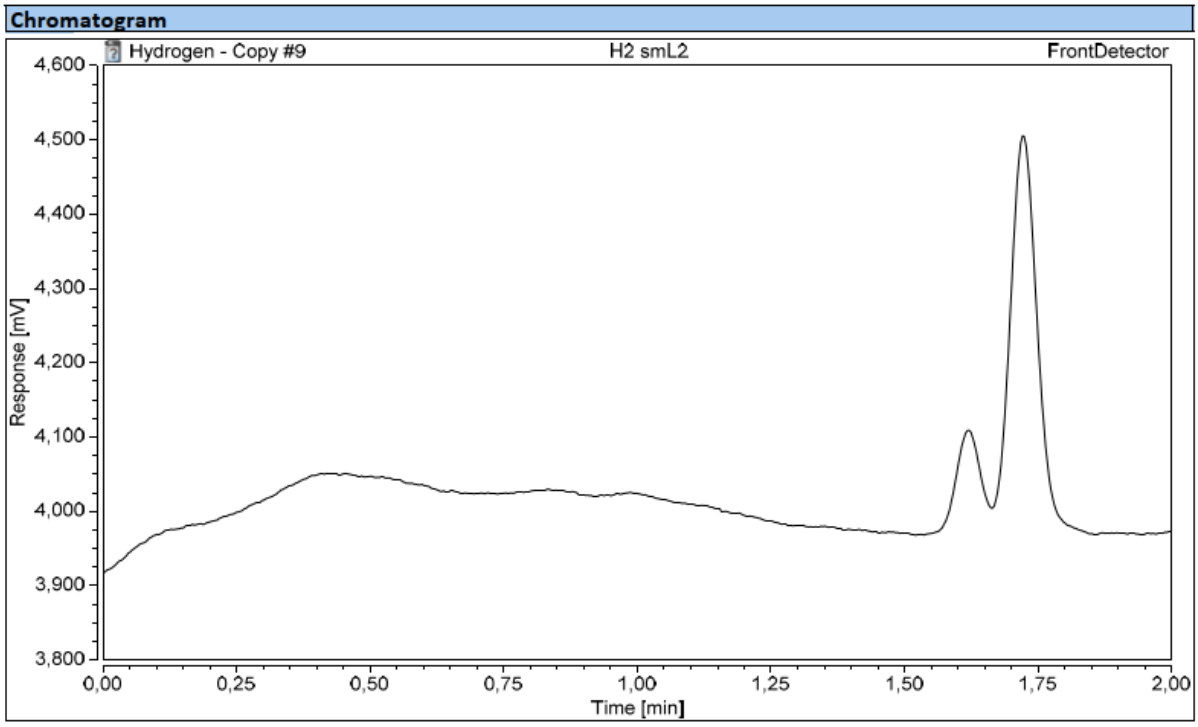

Figure S54. Analysis of gas phase products using GC for the reaction of **SmL** (1 mM) in a CO-purged solution of DMF:H_2O:DIPEA (4:2:1) under blue LED irradiation for 72 h. *This (front-detector) GC trace shows lack of H_2 formation in the reaction.*

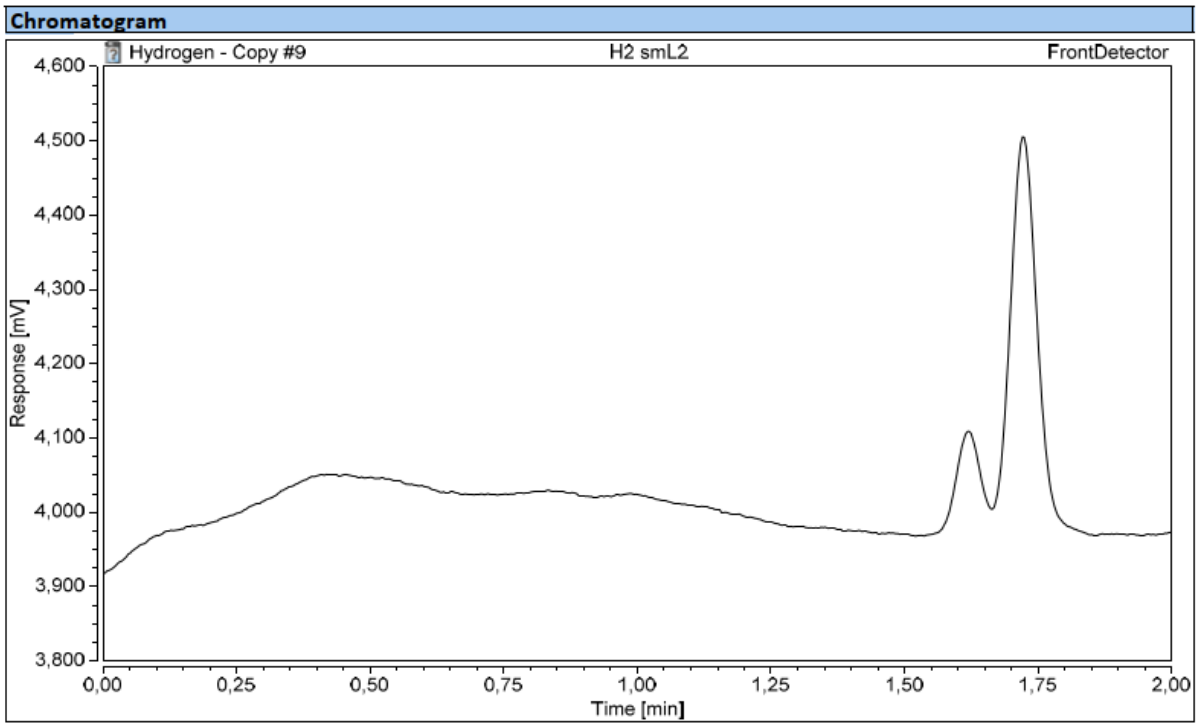

Figure S55. Analysis of gas phase products using GC for the reaction of **SmL** (1 mM) in a CO-purged solution of DMF:H_2O:DIPEA (4:2:1) under blue LED irradiation for 72 h. *This (front-detector) GC trace shows lack of H_2 formation in the reaction.*

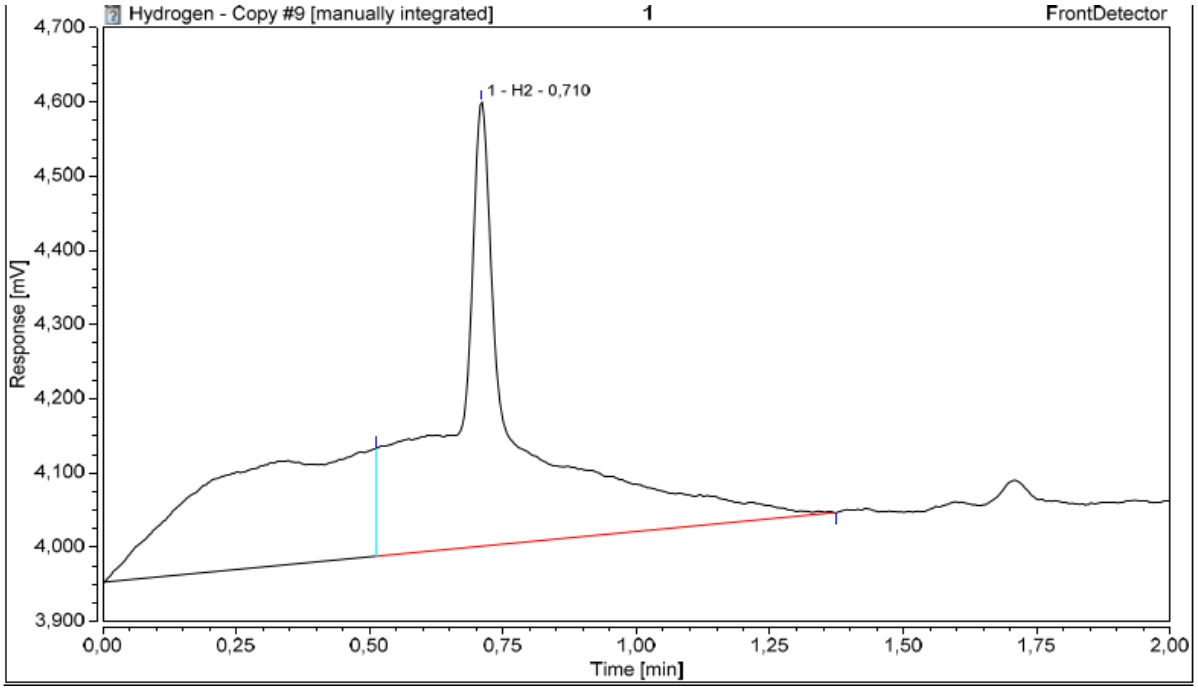

Figure S56. Analysis of gas phase products using GC for the reaction of **SmL** (1 mM) in a CO-purged solution of DMF:H_2O (1:1) under blue LED irradiation for 72 h. *This (front-detector) GC trace shows H_2 formation in the reaction.*

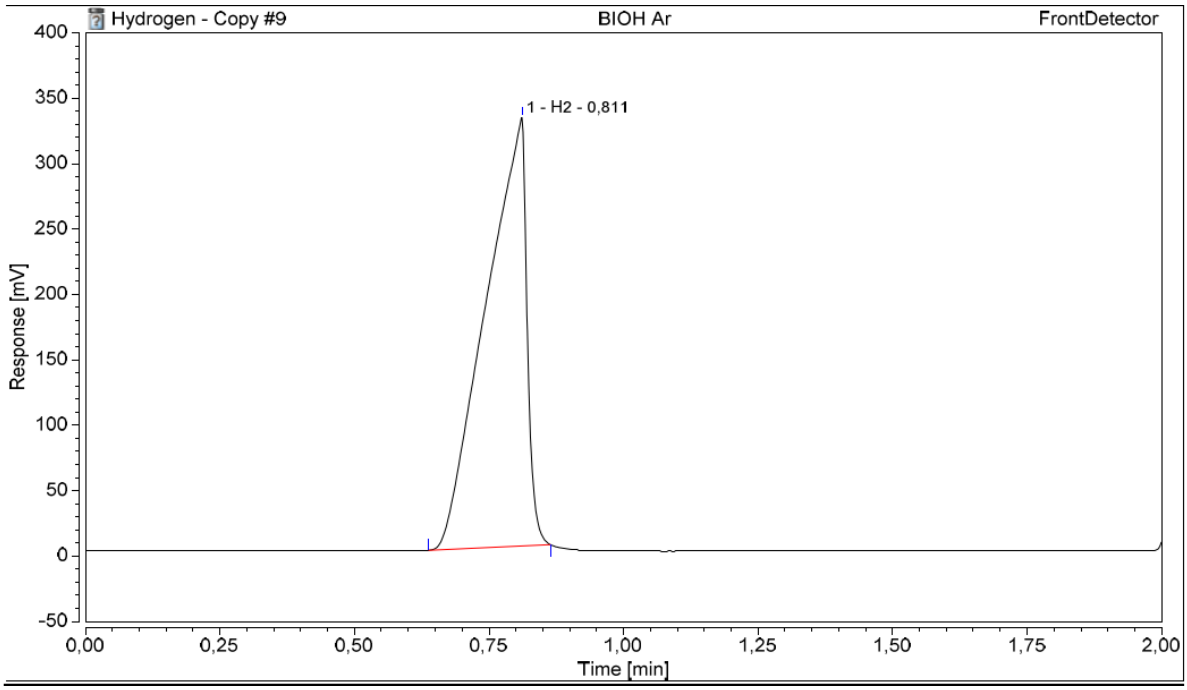

Figure S57. Analysis of gas phase products using GC for the reaction of **SmL** (100 µM) in a Ar-purged solution of DMF:H_2O (1:1) under blue LED irradiation for 48 h.

References

(1) Tomar, M.; Bhimpuria, R.; Kocsi, D.; Thapper, A.; Borbas, K. E. *J. Am. Chem. Soc.* **2023**, *145*, 22555.
(2) Wisser, F. M.; Duguet, M.; Perrinet, Q.; Ghosh, A. C.; Alves-Favaro, M.; Mohr, Y.; Lorentz, C.; Quadrelli, E. A.; Palkovits, R.; Farrusseng, D.; Mellot-Draznieks, C.; de Waele, V.; Canivet, J. *Angew. Chem. Int. Ed.* **2020**, *59*, 5116.
(3) Wang, Y.-F.; Zhang, M.-T. *J. Am. Chem. Soc.* **2022**, *144*, 12459.
(4) Shi, Y.-R.; Lin, R.-Y.; Chen, M.-L.; Dong, X.; Li, H.-Y.; Weng, W.-Z.; Zhou, Z.-H. *J. Mol. Struct.* **2022**, *1254*, 132303.
(5) Yuan, H.; Cheng, B.; Lei, J.; Jiang, L.; Han, Z. *Nat. Commun.* **2021**, *12*, 1835.
(6) Lan, G.; Fan, Y.; Shi, W.; You, E.; Veroneau, S. S.; Lin, W. *Nat. Catal.* **2022**, *5*, 1006.
(7) Hao, Y.-C.; Chen, L.-W.; Li, J.; Guo, Y.; Su, X.; Shu, M.; Zhang, Q.; Gao, W.-Y.; Li, S.; Yu, Z.-L.; Gu, L.; Feng, X.; Yin, A.-X.; Si, R.; Zhang, Y.-W.; Wang, B.; Yan, C.-H. *Nat. Commun.* **2021**, *12*, 2682.
(8) Shirley, H.; Su, X.; Sanjanwala, H.; Talukdar, K.; Jurss, J. W.; Delcamp, J. H. *J. Am. Chem. Soc.* **2019**, *141*, 6617.
(9) Guo, Z.; Chen, G.; Cometto, C.; Ma, B.; Zhao, H.; Groizard, T.; Chen, L.; Fan, H.; Man, W.-L.; Yiu, S.-M.; Lau, K.-C.; Lau, T.-C.; Robert, M. *Nat. Catal.* **2019**, *2*, 801.
(10) Kamada, K.; Jung, J.; Wakabayashi, T.; Sekizawa, K.; Sato, S.; Morikawa, T.; Fukuzumi, S.; Saito, S. *J. Am. Chem. Soc.* **2020**, *142*, 10261.